INFORMATION TO USERS

This manuscript has been reproduced from the microfilm master. UMI films the text directly from the original or copy submitted. Thus, some thesis and dissertation copies are in typewriter face, while others may be from any type of computer printer.

The quality of this reproduction is dependent upon the quality of the copy submitted. Broken or indistinct print, colored or poor quality illustrations and photographs, print bleedthrough, substandard margins, and improper alignment can adversely affect reproduction.

In the unlikely event that the author did not send UMI a complete manuscript and there are missing pages, these will be noted. Also, if unauthorized copyright material had to be removed, a note will indicate the deletion.

Oversize materials (e.g., maps, drawings, charts) are reproduced by sectioning the original, beginning at the upper left-hand corner and continuing from left to right in equal sections with small overlaps. Each original is also photographed in one exposure and is included in reduced form at the back of the book.

Photographs included in the original manuscript have been reproduced xerographically in this copy. Higher quality 6" x 9" black and white photographic prints are available for any photographs or illustrations appearing in this copy for an additional charge. Contact UMI directly to order.

UMI

A Bell & Howell Information Company
300 North Zeeb Road, Ann Arbor MI 48106-1346 USA
313/761-4700 800/521-0600

Performance Analysis and TestBed Demonstration of Long-Haul Point-To-Point Transmission Systems Based On DWDM Technology

by

Maria Fernanda Mendez

A dissertation submitted to the Graduate Faculty in Engineering in partial fulfillment of the requirements for the degree of Doctor of Philosophy, The City University of New York.

1998

Approval Page

This manuscript has been read and accepted for the Graduate Faculty in Engineering in satisfaction of the dissertation requirement for the degree of Doctor of Philosophy.

7/29/98
Date

Chair of Examining Committee

7/29/98
Date

Executive Officer

Prof. M. A. Ali (Mentor)

Prof. Samir A. Ahmed

Prof. Leonid Roytman

Prof. Abraham W. Habib

Jonathan Nagel (AT&T Labs)

THE CITY UNIVERSITY OF NEW YORK

Abstract

Performance Analysis and TestBed Demonstration of Long-Haul Point-To-Point Transmission Systems Based On DWDM Technology

by

Maria Fernanda Mendez

Advisor: Professor Mohamed Ali

This thesis examines the technological requirements and assesses the performance analysis and feasibility for implementing ultra-high bit-rate long-haul point-to-point transmission system based on Dense Wavelength-Division Multiplexing (DWDM) technology. Specifically, this work will develop and demonstrate several ultra-high bit-rate long-haul DWDM transmission system configurations. In these configurations, the number of DWDM channels will vary from 16-100 wavelength at 622 Mb/s, 2.5 Gb/s and 10 Gb/s data rates per channel, giving total system capacities in the order of a Tb/s over a transmission distance of about 600-1200 km with 6-12 spans. To the best of our knowledge, this is the largest DWDM Transmission systems with the highest capacity yet reported.

To realize an ultra-high speed long-haul DWDM transmission system, two key technological issues, that are the focus of this thesis, must be addressed:

- Novel architectures that offer a possible route to ultra-broad band amplifiers capable of providing 60-80 nm of optical bandwidth based on erbium-doped silica fiber must be developed. Using these ultra-broad band EDFAs, the number of WDM channels can then grow to about 80-100 channels while keeping a channel spacing compatible with practical filtering technology.

This work develops and demonstrates several novel two-band EDFA configurations capable of providing as large as 80-nm of optical bandwidth using only silica-based EDFAs. Such configurations offer a practical route to removing the bandwidth limits which currently constrain the design of flexible WDM systems and networks. With 80 nm of bandwidth, this EDFA configuration will be able to accommodate 100 WDM channels with the proposed ITU standard channel spacing of 100 GHz. One of the most important criterion that will be met in designing our proposed EDFA configuration is that it has to be flexible for graceful in-service upgrade to a maximum of 100 WDM channels along with the smooth evolution in increasing the bit rate per channel from OC-12 to OC-192.

Specifically, this work will investigate and develop several ultra wide-band gain-flattened

and stabilized silica-based EDFA configurations with flexible and scalable Wavelength Add/ Drop (WADM) capabilities. The WADM is assumed to be located between the dual-stage EDFA of each band. Each WADM consists of short-period fiber grating filters along with circulators and a given number of wavelength selective elements depending on the number of wavelengths to be added dropped, to perform the WADM capabilities.

- A novel practical filtering technology that is compatible with the channel spacing must also be developed and investigated. Specifically, this thesis compares and examines the potential of both existing and emerging WDM switching technologies and develops a novel WDM filtering technologies using fiber grating filters.

In examining the filtering technology options, the characteristics of filters will be compared based on the following:

- Insertion loss
- Optical bandwidth
- Crosstalk for both adjacent and non adjacent channels
- Polarization dependence loss

The proposed work will be carried out in two overlapping phases: (i) modeling and simu-

lation, and (ii) related experiments. First, we will measure and characterize the performance of a single-stage dual-stage amplifier. We will also measure and fully characterize the performance of a single fiber grating filter by measuring its transmittance and reflectance transfer functions. Then, we will develop a flexible and user-friendly computer modeling tool to investigate the overall performance of several different two-band EDFA architectures with different pumping schemes, pumping wavelength, pumping power, and WADM capabilities. We will then use the initial simulation results for guiding our experimental program, to establish theoretical limits to performance and to compare with experimental results.

The end-to-end performance of these two-band EDFA configurations will then be tested and examined when cascaded in a practical ultra-high speed WDM backbone network. This will be achieved in the context of modeling the end-to-end performance of several DWDM transmission systems. We will implement a flexible, powerful computer modeling tool for evaluating the end-to-end performance of DWDM transmission systems. The tool will include wavelength driven and time driven capabilities. The wavelength driven capability is required to model the effects of cascading many optical amplifiers and optical filters on the output signal to noise ratio and crosstalk level of any signal on the network. The time driven capability is required to model the effects of fiber chromatic and polarization dispersion, crosstalk from adjacent channels, timing jitters due to noise and crosstalk, and non-perfect extinction ratio in external modulators, on the signal quality in the network. The model will relate parameters at

the device-level to system-level performance measures such as bit error rate (BER) and noise margin.

In a DWDM transmission system, an optical signal may pass through many nodes en route to the final destination. Signal degradation can occur at each node due to finite filter pass-bands and filter misalignment, added crosstalk signals, added EFDA amplifier spontaneous emission (ASE) noise, and wavelength dependent gain. The main objective of this work is to investigate the accumulation of these optical degradations in the proposed DWDM transmission systems.

Finally, using the key DWDM enabling technologies developed in this thesis, we will demonstrate and characterize the end-to-end performance of sixteen 2.5 Gb/s DWDM channels transmission over 800 km of standard SMF.

Acknowledgment

"Mami he llegado hasta aqui gracias a ti, te quiero"

This work could not have been done without the guidance and support of my advisor Professor Mohammed Ali, who showed me the road to a challenging career. Stan Lumish (Lucent Technologies), who from the very begining encouraged me to go on and finish with my work, and gave me the flexibility to balance my thesis work and my job. Joe Kunz (Lucent Technologies), even though it was for a short time, but you supported my studies while I was under your supervision. Bill Gartner and Raj V. (Lucent Technologies) thanks for making my decision easier at a crucial time in my life. Nat Denkin (Lucent Technologies) thanks for being an annoying uncle and for looking out for me in times of distress. Dirk Bode (Lucent Technologies) for his incredible support and tutoring on the amplifier configurations and experiment setups. Bernhard Schmauss (Lucent Technologies) for his tutoring on the simulation tool. Hector for being such a great friend and fan. And finally, to all my friends because I know you all will be throwing me the biggest party ever.

Table of Contents

CHAPTER 1 *Introduction 1*

Introduction 1
Thesis Statement 6

CHAPTER 2 *Critical Technologies for Long-Haul Point-to-Point Transmission Systems 13*

Introduction 13
Dense WDM System Overview 15
Key Enabling Technologies 17
Fiber Optical Amplifiers 17
WDM Transmitter Considerations for Long Amplified Fiber Optic Systems 20
DWDM Receiver Characteristics 24
DWDM Filter Components 27

CHAPTER 3 *Development and Characterization of the Two Key Enabling Technologies 31*

Introduction 31
Novel Wideband High Output Power EDFA Configurations 32
Fundamentals of Optical Amplifiers 32
Comparison of Experiment and Simulation of Optical Amplifiers 35
Mux Dmux Compatible with 50/100 Ghz Channel Spacing 49
Introduction 49
Design Considerations of Large-Number and Narrow Channel Spacing DMUX 49
Thin-Film Filter Technology 56
Fiber Grating Technology 58

CHAPTER 4 *16 x 2.5 Gbit/s DWDM Transmission System Demonstration* **62**

Introduction **62**
Experimental Results **63**
Simulation Results **67**

CHAPTER 5 *Feasibility of Tb/s DWDM Transmission Systems* **69**

Introduction **69**
Two-Band Silica-Based EDFAs Architectures **73**
Modeling the Two-Band EDFA Configuration *75*
64 100 x 10 Gbit/s DWDM Transmission System with 50 and or 100 Ghz Channel Spacing **76**
Introduction *76*
The System Model *77*
Results and Discussion *79*
64x2.5 Gb/s DWDM Transmission System With 50 Ghz Channel Spacing **81**
Introduction *82*
The System Model *83*
Results and Discussion *86*

CHAPTER 6 *Conclusion* **99**

Conclusion **99**

CHAPTER 7 *Bibliography* **104**

Chapter 1 **104**
Chapter 2 **105**
Chapter 3 **108**
Chapter 4 **109**
Chapter 5 **109**

List of Figures

Figure 2.1	DWDM Transmission System	16
Figure 2.2	Optical amplifier gain spectra	19
Figure 2.3	Directly modulated lasers vs. externally modulated lasers	21
Figure 2.4	Receiver for optically amplified systems	24
Figure 2.5	Optical Mux/Dmux waveguide filter	30
Figure 3.1	EDFA bidirectional pumping configuration	32
Figure 3.2	Energy level diagram for a 3-level system	33
Figure 3.3	Measurement setup for gain flatness measurement	37
Figure 3.4	Configuration of single stage OA	39
Figure 3.5	Parameters in Simulation of EDFA-Model for Single-Stage OA	40
Figure 3.6	Gain of Single-Stage OA with 20m Er Fiber and P_{in}= -17dBm	41
Figure 3.7	Gain of Single-Stage OA with 20m Er Fiber and	

	P_{in}= -6dBm	42
Figure 3.8	Gain of Single-Stage OA with 12m Er Fiber and P_{in}= -17dBm	43
Figure 3.9	Gain of Single-Stage OA with 12m Er Fiber and P_{in}= -6dBm	44
Figure 3.10	Configuration of Double-Stage OA	45
Figure 3.11	Parameters in Simulation of EDFA-Model for Double-Stage OA	45
Figure 3.12	Gain of Double-Stage OA with 12/16m Er Fiber and P_{in}= -17dBm	47
Figure 3.13	Gain of Double-Stage OA with 12/16m Er Fiber and P_{in}= -6dBm	48
Figure 3.14(a)	The worst case wavelength detuning between signal and DMUX for a peaked router	51
Figure 3.14(b)	The worst case wavelength detuning between signal and	

	DMUX for a flat-top router	52
Figure 3.15	Schematic drawing of the PAW router. R = Slab-coupler focal length. d = Grating pitch	54
Figure 3.16	Structure of a multilayer interference cavity thin film based multiplexer	57
Figure 3.17	Writing a fiber bragg grating	59
Figure 3.18	(a) Transmission and (b) reflection spectra of a fiber bragg grating	60
Figure 3.19	Applications of fiber gratings	61
Figure 4.1	Experimental setup of 16 x 2.5 Gbit/s Transmission System	64
Figure 4.2	Experimental results of 16 x 2.5 Gbit/s over 800 Km transmission system	66
Figure 4.3	Simulation vs. Measurement results. M8x25: Measurement after 9th OA with 25 dB span loss.	

	D8x25: Simulation after 9th OA with 25 dB span loss	68
Figure 5.1	Schematic diagram of one architecture of proposed dual-band EDFA	89
Figure 5.2	Add/Drop design for 51 λ	90
Figure 5.3	51 λ Add/Drop	91
Figure 5.4	Bidirectional schematic diagram of a second architecture of proposed dual-band EDFA configuration using only one fiber	92
Figure 5.5	Two overlapped transmission spectra of broadband bragg fiber gratings used in ultra-broadband EDFA configurations. The transition region between reflection of the S-band and the transmission of the L-band is about 0.5 nm	93
Figure 5.6	Two-band EDFA configuration	94
Figure 5.7	(a) Output power after the 1st EDFA. (b) Output power	

	after the 11th EDFA	95
Figure 5.8	Two system configurations for the transmission of 64 channels at 50 Ghz channel spacing	96
Figure 5.9	Transmission characteristics of a long-period fiber grating	97
Figure 5.10	Spectra after 1st and 12th EDFA (0.2 nm resolution)	98

CHAPTER 1 *Introduction*

1.1 Introduction

Over the past few years, the field of computer and telecommunications networking has experienced tremendous growth. With the rapidly growing popularity of the Internet and the World Wide Web and with the recent deregulation of the telecommunications industry, this growth can be expected to continue in the foreseeable future. The next ten years may bring to the home and office multiple connections of high-definition television, video mail, and digital audio, as well as full Internet connections via user-friendly graphic user interfaces. As more users start to use data networks, and as their usage patterns evolve to include more bandwidth-intensive networking applications, there emerges an acute need for very high bandwidth trans-

port networks facilities whose capabilities greatly exceed those of current high-speed networks. This has created a growing realization of the need for dramatically upgrading the information infrastructure, both on the national and local access levels.

Data communication networks capable of supporting Tb/s applications over both local area and wide area must overcome key bottlenecks imposed by technological limitations. Electronics bottlenecks are imposed by a maximum capacity limit in the region of a few tens of Gb/sec and by the components needed for serialization, deserialization, and clock recovery. Photonics bottlenecks arise from the photodetector bandwidth, limited wavelength tuning range, relatively slow tuning times, insufficient wavelength stability, and lack of optical buffering. Consequently, these technological bottlenecks, have impeded the efficient use of the enormous bandwidth inherent in optical fibers. To solve these technological bottlenecks, and to advance the communication link toward exploiting the huge optical fiber capacity, a multi-channel transmission scheme is needed, with each channel running at about the capacity of electronics, i.e., several to few tens of Gb/s.

The key to upgrading such an infrastructure rests in the relatively young field of fiber optics. Given that fiber has a potential bandwidth of approximately 50 Tb/s, nearly four order of magnitude higher than peak electronic data rates, every effort should be made to tap into the capabilities of fiber-optic networks. Multi-channel networks can be implemented using

optical fibers through dense wavelength-division multiplexing (DWDM), subcarrier multiplexing (SCM), time-division multiplexing (TDM), code-division multiple access (CDMA), or a combination of these techniques.

One of the most powerful multiplexing techniques for accessing the huge bandwidth available in an optical fiber is dense wavelength-division multiplexing (DWDM). In DWDM, the optical transmission spectrum is divided into a number of nonoverlapping wavelength bands, with each wavelength supporting a single communication channel operating at peak electronic speed. Multiple numbers of these channels can then be transported through a single fiber, thus tapping into the huge fiber bandwidth. The challenge is to design and develop appropriate network architectures, components, protocols, and algorithms, that is the research focus of this proposal, to support such a system.

The use of WDM technology provides a powerful mechanism to overcome these technological bottlenecks while preserving the important survivability feature. This is particularly true when transmission and wavelength assignment are performed in a manner that does not require each terminal to detect and process all wavelengths traveling through transmission path. The transparency and independence of the WDM channels permit vastly dissimilar bit rates to pass between different pairs of nodes, allowing network connectivity and transmission rates to be tailored and upgraded flexibly according to prevailing traffic patterns and evolving

service demands. Unlike single-channel TDM systems, DWDM systems effectively use the large built-in bandwidth in installed fibers while maintaining the same or greater degrees of system performance, robustness, reliability, operations, and maintenance as current transport systems.

A DWDM system is constituted of several key elements such as: WDM terminals (transmitters and receivers), WDM repeaters, e.g., Erbium-doped fiber amplifiers (EFDAs), and WDM filters. Optical amplifiers can simultaneously accommodate multiple optical channels and therefore have greatly accelerated the pace at which WDM systems are being developed and deployed. Important to the effectiveness of this system are high performance transmitters and receivers. Many challenges are encountered in the design of these devices to ensure high quality transmission in DWDM systems. In addition, low loss, high resolution WDM filters are also crucial for DWDM communication systems.

The prospects for creating such DWDM transmission systems that are transparent to signal format and bit rate are being investigated in several consortia activities and research programs around the world. The principle goal for these programs is to create the possibility of a "future proof" network in which the optical signals flowing through the network are uninterrupted by electronics from source to destination, and in which the character of the individual signals is determined by the terminal equipment which is attached to the network at the source

and destination. DWDM optical fiber communication systems with 20 Gb/s capacity (8-channels each with 2.5 Gb/s) are being deployed on commercial networks (AT&T News, July 1995).

The design of DWDM systems and optical networks is currently constrained by the limited bandwidth available from erbium-doped fiber amplifiers (EDFAs). The usable bandwidth is limited to about 12-nm because of the highly structured gain spectrum. With gain equalization filters (GEFs) [1], this gain bandwidth can be extended to between 35 and 40 nm (about 1525 to about 1565 nm) [2-3]. Since the gain drops sharply below 1525 nm or above 1565 nm, it is not practical to further increase the gain bandwidth with GEFs. As we scale up the number of wavelengths in WDM systems, the spacing between wavelengths will decrease and the crosstalk among channels will increase. This system crosstalk will eventually limit the scaling capacity of WDM networks required for the efficient implementation of the Next-Generation Internet (NGI) backbone transport facilities. In addition, current long haul WDM transport systems have very limited wavelength add/drop (WADM) capabilities, which is a key limiting factor hindering the feasibility of creating robust and flexible WDM systems.

To further increase capacity with a channel spacing compatible with practical filtering technology, as well as to increase wavelength routing network capability, the number of channels must grow. It would also be advantageous to be able to access one or more of the optical

channels at any amplifier site in a WADM configuration. The WADM configuration must include both fixed and reconfigurable optical add/drop multiplexers. This will require developing novel ultra broad-band silica-based EDFA configurations with flexible and scalable optical add/drop capabilities along with a compatible filtering technology, that is the focus of this thesis, capable of providing 60-80 nm of optical bandwidth while keeping both the spectral gain variations and the inter-channel cross-talk as small as possible. These capabilities are essential for pushing broad-band access to the end users and provide a credible starting point for achieving the objectives of the NGI initiative.

1.2 Thesis Statement

This thesis examines the technological requirements and assesses the performance analysis and feasibility for implementing very high bit-rate long-haul point-to-point transmission system based on DWDM technology. Specifically, this work will develop and demonstrate several very high bit-rate long-haul DWDM transmission system configurations. In these configurations, the number of DWDM channels will vary from 16-100 wavelength at 622 Mb/s, 2.5 Gb/s and 10 Gb/s data rates per channel, giving total system capacities in the order of a Tb/s over a transmission distance of about 600-1200 km with 6-12 spans. To the best of our knowledge, this is the largest DWDM Transmission systems with the highest capacity yet

reported.

To realize an ultra-high speed long-haul DWDM transmission system, two key technological issues need to be addressed:

1. Novel architectures that offer a possible route to ultra-broad band amplifiers capable of providing 60-80 nm of optical bandwidth based on erbium-doped silica fiber must be developed. Using these ultra-broad band EDFAs, the number of WDM channels can then grow to about 80-100 channels while keeping a channel spacing compatible with practical filtering technology.

One possible solution for broad-band EDFAs is achieved using new materials. Erbium-doped fluoride fibers have been shown to provide a gain bandwidth of 24 nm without GEF [4]. Erbium-doped tellurite fibers have also been reported to be a promising candidate [5]. However, the gain spectrum of tellurite EDF is highly non-uniform and many other properties need to be investigated before such fibers can be qualified for practical applications. Alternatively, new architectures offer a possible route to broad band amplifiers based on erbium-doped silica fiber. Previous work has shown that optical gain can be obtained in erbium-doped silica fibers in the long wavelength range between 1570 and 1600 nm (called L-band here) [6-7].

This work develops and demonstrates several novel two-band EDFA configurations capa-

ble of providing as large as 80-nm of optical bandwidth using only silica-based EDFAs. This is achieved by combining the gain in the conventional wavelength range between 1525 and 1565 nm (called S-band in this work) and that in the long wavelength range between 1570 and 1600 nm (called L-band here). Each configuration consists of two parallel dual-stage silica-based EDFA, where each dual-stage is independently optimized. Such configurations offer a practical route to removing the bandwidth limits which currently constrain the design of flexible WDM systems and networks. With 80 nm of bandwidth, this EDFA configuration will be able to accommodate 100 WDM channels with the proposed ITU standard channel spacing of 100 GHz. One of the most important criterion that will be met in designing our proposed EDFA configuration is that it has to be flexible for graceful in-service upgrade to a maximum of 100 WDM channels along with the smooth evolution in increasing the bit rate per channel from OC-12 to OC-192.

Specifically, this work will investigate and develop several ultra wide-band gain-flattened and stabilized silica-based EDFA configurations with flexible and scalable Wavelength Add/Drop (WADM) capabilities. The WADM is assumed to be located between the dual-stage EDFA of each band. Each WADM consists of fiber grating filters along with circulators and a given number of wavelength selective elements depending on the number of wavelengths to be added/dropped, to perform the WADM capabilities. These configurations must be capable of satisfying the following:

- Low-noise and high output power.
- Gain flatness should be independent of the operating conditions (signal and pump power levels, etc.).
- Maintain constant per-channel output power with a minimally degraded SNR, regardless of the number of channels present, over a wide dynamic range of input signal levels.
- Amplify and add/drop any number of wavelengths ranging from 1-100.
- Flexible for graceful in-service upgrade to a maximum of 100 WDM channels along with the smooth evolution in increasing the bit rate per channel from OC-12 to OC-192.

We will examine the various technological difficulties facing EDFA cascades with multi-wavelength handling capabilities. Two related fundamental problems will be addressed:

(i) spectral gain non-uniformity or "gain equalization". This is one of the major remaining problems facing multiwavelength transmission systems with fiber-amplifier cascades. When wavelength-multiplexed signals traverse a single amplifier, the individual channels experie. ce various gains determined by the spectroscopy of the gain medium, the fiber length, and the signal and pump power levels. In a single amplifier, these spectral gain variations are generally modest, but they accumulate from stage to stage in a cascade, rapidly growing too large to allow adequate noise performance at the less-favored signal wavelengths.

(ii) noise accumulation in high data rate WDM repeater chains.

The main objective is to ensure sufficient gain flatness to permit amplifiers to be cascaded while maintaining acceptable inter channel power variations and signal-to-noise ratios at all wavelengths. The feasibility of using two new features, crucial for broadband long-haul DWDM transmission systems, to equalize (flatten) the passband of cascaded EDFAs will be examined. First, long-period fiber gratings will be used to flatten the gain and broaden the optical bandwidth of a two-stage mid-amplifier pumped EDFAs. Second, mid-amplifier attenuators will be used to permit the EDFAs to be operated with broadband, flat gain over a wide dynamic range of input powers which is necessary to accommodate variations encountered in system span losses.

2. A novel practical filtering technology that is compatible with the channel spacing must also be developed and investigated. Specifically, this thesis compares and examines the potential of both existing and emerging WDM switching technologies and develops a novel WDM switching technologies using long/short period fiber grating filters.

In examining the filtering technology options, the characteristics of filters will be compared based on the following:

- Insertion loss
- Optical bandwidth

- Crosstalk for both adjacent and non adjacent channels
- Polarization dependence loss

The proposed work will be carried out in two overlapping phases: (i) modeling and simulation, and (ii) related experiments. First, we will measure and characterize the performance of a single-stage/dual-stage amplifier. We will also measure and fully characterize the performance of a single short/long-period grating filter by measuring its transmittance and reflectance transfer functions. Then, we will develop a flexible and user-friendly computer modeling tool to investigate the overall performance of several different two-band EDFA architectures with different pumping schemes, pumping wavelength, pumping power, and WADM capabilities. We will then use the initial simulation results for guiding our experimental program, to establish theoretical limits to performance and to compare with experimental results.

The end-to-end performance of these two-band EDFA configurations will then be tested and examined when cascaded in a practical ultra-high speed WDM backbone network. This will be achieved in the context of modeling the end-to-end performance of several DWDM transmission systems. We will implement a flexible, powerful computer modeling tool for evaluating the end-to-end performance of DWDM transmission systems. The tool will include wavelength driven and time driven capabilities. The wavelength driven capability is

required to model the effects of cascading many optical amplifiers and optical filters on the output signal to noise ratio and crosstalk level of any signal on the network. The time driven capability is required to model the effects of fiber chromatic and polarization dispersion, crosstalk from adjacent channels, timing jitters due to noise and crosstalk, and non-perfect extinction ratio in external modulators, on the signal quality in the network. The model will relate parameters at the device-level to system-level performance measures such as bit error rate (BER) and noise margin.

In a DWDM transmission system, an optical signal may pass through many nodes en route to the final destination. Signal degradation can occur at each node due to finite filter pass-bands and filter misalignment, added crosstalk signals, added EFDA amplifier spontaneous emission (ASE) noise, and wavelength dependent gain. The main objective of this work is to investigate the accumulation of these optical degradations in the proposed DWDM transmission systems.

Finally, using the key DWDM enabling technologies developed in this thesis, we will demonstrate and characterize the end-to-end performance of sixteen 2.5 Gb/s DWDM channels transmission over 800 km of standard SMF.

CHAPTER 2

Critical Technologies for Long-Haul Point-to-Point Transmission Systems

2.1 Introduction

One of the most powerful multiplexing techniques for accessing the huge bandwidth available in an optical fiber is dense wavelength-division multiplexing (DWDM). In DWDM, the optical transmission spectrum is divided into a number of nonoverlapping wavelength bands, with each wavelength supporting a single communication channel operating at peak electronic speed. Multiple numbers of these channels can then be transported through a single fiber, thus tapping into the huge fiber bandwidth. The challenge is to design and develop appropriate network architectures, components, protocols, and algorithms, that is the research focus of this proposal, to support such a system.

The use of WDM technology provides a powerful mechanism to overcome these technological bottlenecks while preserving the important survivability feature. This is particularly true when transmission and wavelength assignment are performed in a manner that does not require each terminal to detect and process all wavelengths traveling through transmission path. The transparency and independence of the WDM channels permit vastly dissimilar bit rates to pass between different pairs of nodes, allowing network connectivity and transmission rates to be tailored and upgraded flexibly according to prevailing traffic patterns and evolving service demands. Unlike single-channel TDM systems, DWDM systems effectively use the large built-in bandwidth in installed fibers while maintaining the same or greater degrees of system performance, robustness, reliability, operations, and maintenance as current transport systems.

Unlike single-channel TDM systems, DWDM systems effectively use the large built-in bandwidth in installed fibers while maintaining the same or greater degrees of system performance, robustness, reliability, operations and maintenance as current transport systems. A DWDM system is constituted of several key elements such as: Erbium-doped fiber amplifiers, transmitters, receivers, and WDM filters. Optical amplifiers can simultaneously accommodate multiple optical channels and therefore have greatly accelerated the pace at which wavelength division multiplexing (WDM) systems are being developed and deployed. Important to the effectiveness of this system are the high performance transmitters and receivers. Many chal-

lenges are encountered in the design of these devices to ensure high quality transmission in DWDM systems. In addition, low loss, high resolution WDM filters are also crucial for DWDM communications systems. The following sections present an overview of DWDM systems and basic theory and technologies of the components used in the systems.

2.2 *Dense WDM System Overview*

A DWDM system, as illustrated in figure 2.1, is a flexible high capacity lightwave system that multiplexes the digitally encoded signals at 2.5 Gb/s and sends the resulting signal through optical fibers. Depending on the traveling distances the use of in-line optical repeaters is needed for the re-amplification of the signal to be demultiplexed at the other end.

Currently, a DWDM system requires an optical repeater approximately every 120 Km to re-amplify signals. The distance between end terminals and adjacent optical repeaters or between adjacent repeaters is called an optical section or span. The DWDM can transmit over several types of fiber, Standard Single Mode Fiber (SSMF), Non-Zero Dispersion Fiber (NZDF), and Dispersion Shifted Fiber (DSF) and supports distances of approximately 1000 Km without optoelectronical regeneration of signals.

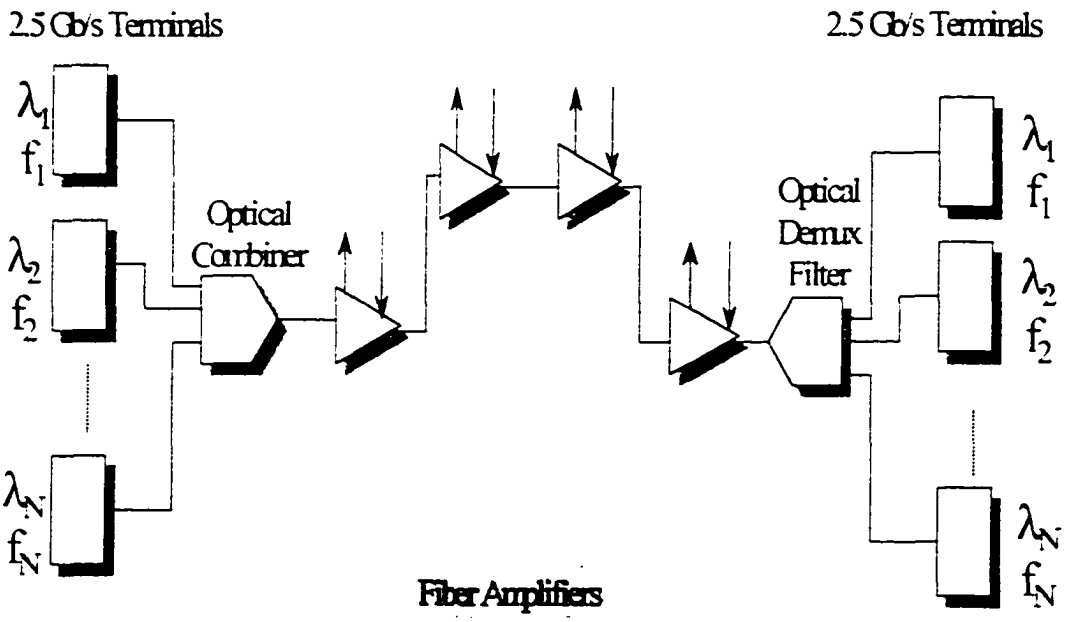

Figure 2.1. DWDM Transmission System

The erbium-doped fiber optical amplifiers can simultaneously amplify several different wavelengths in the 1.5 μm wavelength region [1]. The high gain, high output fiber amplifiers can provide sufficient power to accommodate longer spans, making the system cost effective by annulling electronic repeaters in spans between terminal sites. Optimization of optical signal to noise ratio is achieved by gain equalization techniques, and the multiplexer and demultiplexer units can provide dense wavelength division multiplexing for up to one hundred wavelengths with 50 and 100 GHz optical channel spacing.

2.3 *Key Enabling Technologies*

2.3.1 Fiber Optical Amplifiers

A basic optical amplifier consists of a short length of optical fiber doped with erbium ions and a semiconductor laser at either 980 nm or 1480 nm that pumps the erbium ions to excited states to provide gain in the 1.55 μm communication window. Optical amplifiers can directly amplify lightwave signals, eliminating the need of OE and EO conversions. This simple and elegant function, which is independent of data rate, has revolutionized almost all aspects of lightwave communication systems.

Er^{3+}: silica glass can be modeled as a three-level laser system and its signal gain coefficient is given by

$$g(\lambda) = \sigma_e(\lambda).N_2 - \sigma_a(\lambda).N_1$$

where $\sigma_e(\lambda)$ and $\sigma_a(\lambda)$ are the emission and absorption cross sections of the transition at λ, and N_1 and N_2 are Er^{3+} populations in energy states 1 and 2. Population inversion factor D is defined by

$$D = N_2 - N_1 / N_2 - N_1$$

D = -1 corresponds to the unpumped case of all Er^{3+} ions being in the ground state, and D = 1 corresponds to the case where the system is fully excited, i.e. all ions are in the excited state. Figure 2.2 shows the spectral characteristics of gain coefficient for various inversion levels.

As illustrated in the figure, an unsaturated optical amplifier has a gain bandwidth of > 50 nm. However, the useful gain spectrum narrows considerably in lightwave system applications where the input signals depletes the excited state population and therefore decreases the inversion factor D.

Additionally, when a number of amplifiers are concatenated in a long-haul transmission system, the effective gain of the entire amplifier chain further narrows as a result of accumulation of spectral gain variations. In WDM transmission systems, this effect could lead to unacceptable differences in received channel power, or in extreme cases, a complete power extinction for certain channels. In designing our systems, channels are placed densely in a

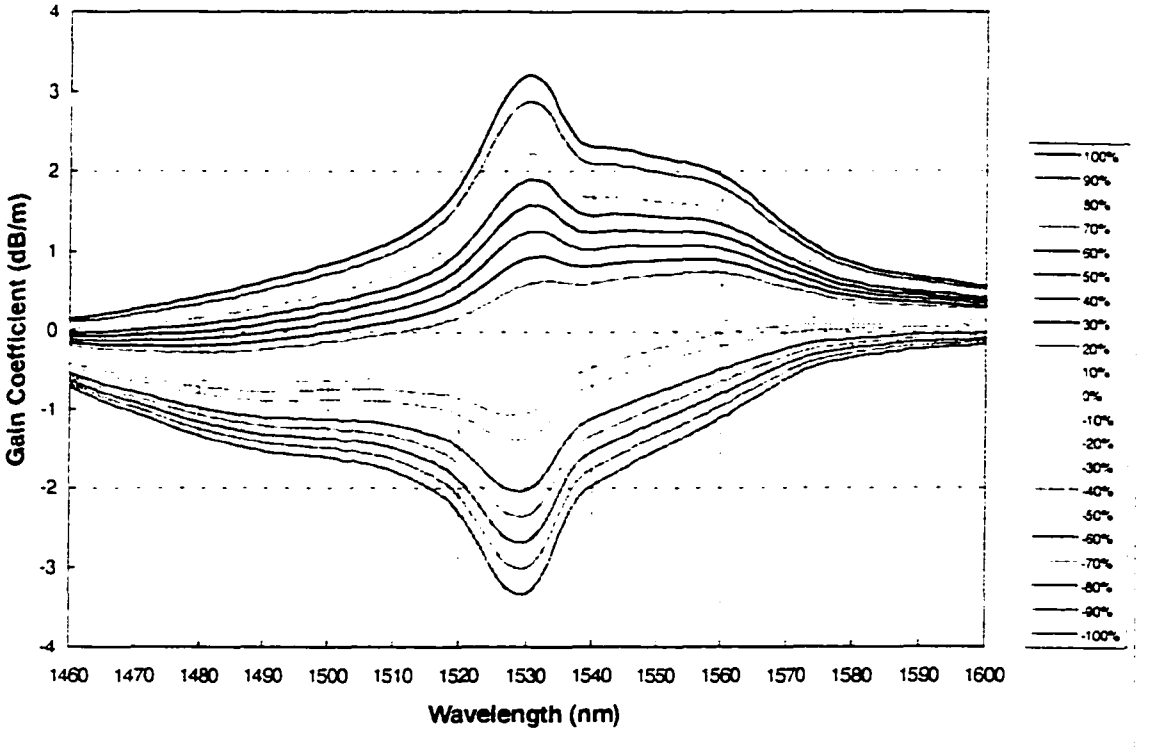

Figure 2.2. Optical Amplifier Gain Spectra

carefully-selected spectral region where the optical amplifiers exhibit the least amount of gain variations. We also employ equalization schemes using long-period fiber grating filters to combat the gain narrowing effect.

Optical amplifiers are used in the WDM system as power boosters, in-line amplifiers and pre-amplifiers. Novel optical amplifier configurations have been developed to optimize system performance in terms of OSNR and fiber nonlinearities. These amplifiers are designed in

such a way that achieve an OSNR high enough to meet the receiver requirement and a power level low enough not to exceed the threshold set forth by fiber self-phase modulation.

With all the features described in this section, the optical amplifiers provide an optical pipe that is truly transparent to number of channels and channel data rates.

2.3.2 WDM Transmitter Considerations for Long Amplified Fiber Optic Systems

In long amplified systems the presence of Amplified Spontaneous Emission (ASE) noise [2,3], multiple optical reflections [4], and large amounts of dispersion have made transmitter design more challenging as designs must now address these additional degradations. In addition, the design of a high performance laser transmitter must include careful consideration of laser reliability, thermal and mechanical design, circuit design, and manufacturability, to name a few.

In the 1550 nm regime the loss is typically less than 0.25 dB/Km, with a dispersion of 17 ps/nm-Km. Presently most 2.5 Gb/s 1550 nm laser transmitters utilize low chirp directly modulated MQW-DFB lasers, since they are generally more available, cheaper, and have higher optical power than externally modulated lasers (see figure 2.3). In some cases the directly

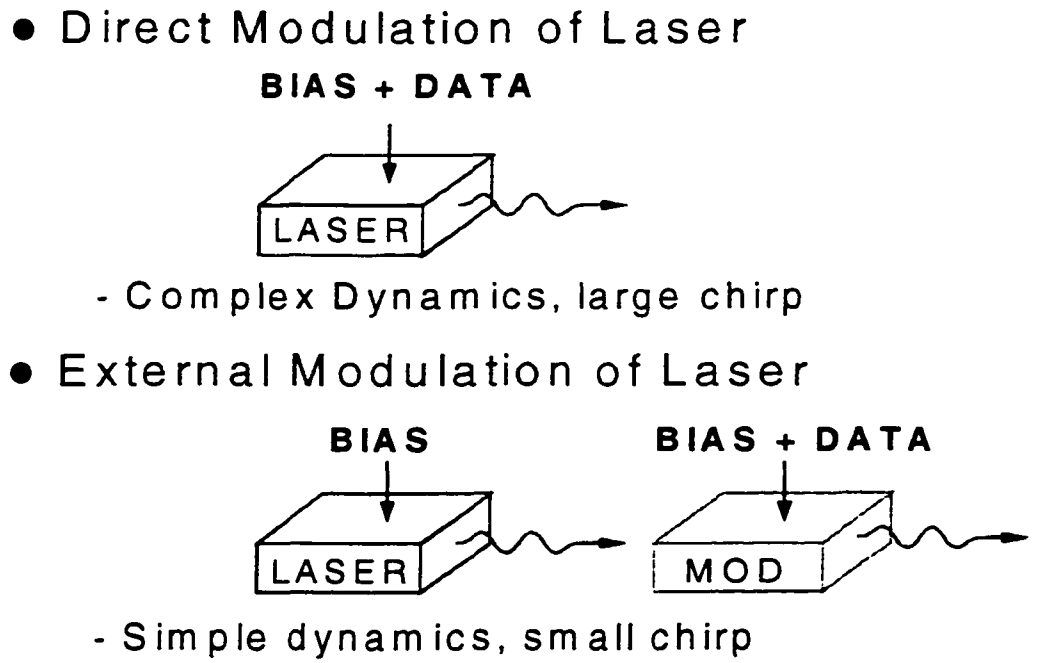

Figure 2.3. Directly modulated lasers vs. externally modulated lasers

modulated 1550 nm DFB lasers have been capable of transmission through more than 160 Km of standard single mode fiber [5]. On the other hand, transmission distances of more than 670 Km have been achieved using an integrated laser and electroabsorption modulator transmitter [6], and 710 Km with a laser modulated with a $LiNbO_3$ Mach-Zehnder modulator which is designed to have virtually no pattern dependent chirp. These transmitters are said to have "transform limited pulses", where the effective laser linewidth, Δv, is limited by the pulse width T, where $\Delta v\ T <= 1$. This will ultimately limit the transmission distance to approximately 1200 Km at 2.5 Gb/s in standard single mode fiber [7].

There are three major transmitter characteristics that are important in the selection of multi-gigabit laser transmitters used in intensity modulated/direct detection systems.

- What is the minimum acceptable extinction ratio for the system application?
- What are the requirements for the modulated pulse shape?
- How much pulse distortion can be tolerated?

In the paragraphs below one of the most important design characteristics, wavelength chirp, will be discussed in greater detail.

Laser chirping will result in pulse distortions at the receiver that are proportional to the total fiber dispersion, the peak-to-peak wavelength chirp, and the duration and location of the chirp. Generally, these pulse distortions limit the transmission distance. However, in amplified systems the effect of fiber non-linearities, particularly self-phase-modulation, can alter the pulses in such a way as to cancel the chirp depending on the polarity of α_{eff} and the dispersion coefficient [8,9]. If carefully controlled this results in improved system performance.

One of the more challenging aspects in designing laser transmitters for long multi-gigabit systems is the difficulty in specifying a laser parameter that correlates well with the dispersion penalty. It is now known that the time-averaged laser spectrum has little to do with the ultimate fiber performance in systems with chromatic dispersion [See for example CCITT Rec-

ommendation G.957 ITU-T Laser Chirp Correspondence Group: Contribution from Telecom Australia 21/7/93].

Alternatively, time-resolved chirp measurements (TRCM) have been used to characterize directly [10], and externally modulated lasers. TRCM provides a bit-by-bit measurement of the pattern dependent instantaneous laser chirp. The use of TRCM to characterize lasers for use in highly dispersive systems is gaining popularity [11,12]. The time resolved chirp data has been correlated to measured dispersion penalties, and thus is a good method of selecting lasers that will operate in highly dispersive fiber.

To take full advantage of the EDFA optical bandwidth, it is essential that the channel spacing be as small as possible. Systems that have up to eight 2.5 Gb/s channels are being deployed on commercial networks [AT&T News, July 1995]. When considering the number of transmitters per fiber pair, and the necessity of having spares, we find that key to the success of multi-channel systems is the availability of low cost laser transmitters. This precludes lasers that rely on optical references for stabilization, or external-cavity lasers. Alternatively, DFB lasers have exhibited wavelength aging characteristics of less than 0.25 nm for 25 years of aging [13,14,15]. Hence, laser transmitters based on DFB lasers, tuned to the desired channel frequency and then temperature controlled, are the best candidates for WDM systems.

2.3.3 DWDM Receiver Characteristics

The receiver in DWDM systems must detect and convert information in optical form to electrical form with minimum influence in the content of the transmitted data. For optically amplified systems, a receiver which will produce the minimum BER while tolerating the noise and distortion typically of such systems is imperative [16]. A receiver must optimize sensitivity, Q factor, dynamic range etc. while keeping a low BER.

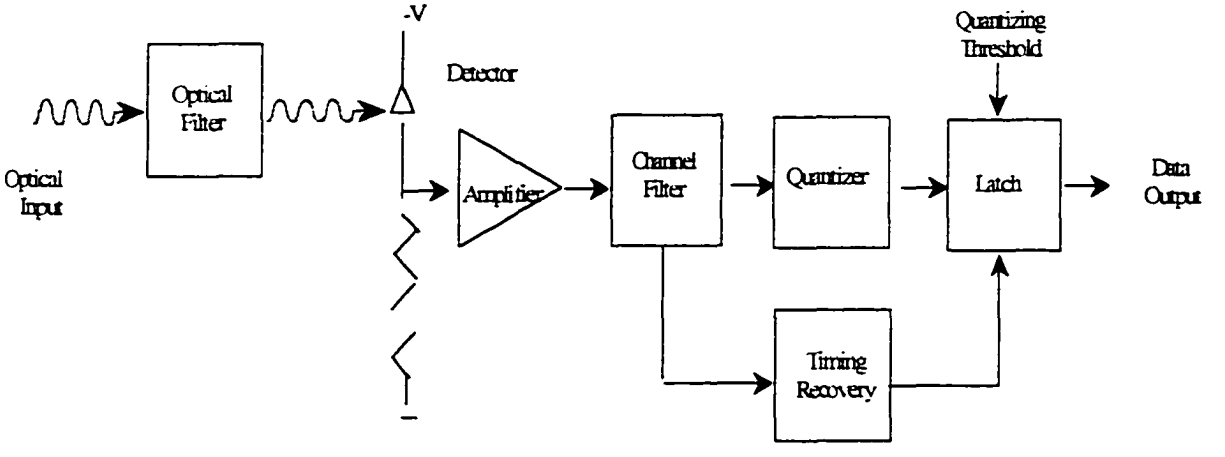

Figure 2.4. Receiver for Optically Amplified Systems

Figure 2.4. shows the topology of a typical receiver for optically amplified systems. The receiver consists of seven parts:

1. **Optical Filter** - The optical filter reduces the incoming ASE noise from the amplifier chain arriving at the receiver.
2. **Detector** - Converts the optical signal into an electrical signal. A photodiode is used (PIN or APD) with square law detection characteristic. The square law characteristic creates baseband information signals that contain the information modulated onto the carrier by the transmitter as well as the noise and distortion added by the transmission system.
3. **Amplifier** - The amplifier provides gain and band shaping to the signals from the detector. Important in an amplifier is to have flat gain and linear phase response.
4. **Channel Filter** - The channel filter equalizes the channel by compensating for the band shapes of the detector and amplifier. This will produce a channel shape that will minimize Inter-Symbol Interference (ISI) and will maximize the SNR at the quantizer.
5. **Quantizer** - The quantizer combines high gain and large fast rates to quantize into two distinct amplitudes data from the channel filter. Input voltages above a pre-determined threshold are considered marks or "1" and below the threshold are considered spaces or "0". In an amplified system, the BER is determined in the quantizer because errors due to amplitude variations (such as those created by system noise and ISI) are more significant than those due to timing effects (such as jitter).
6. **Timing Recovery** - The timing recovery circuit recovers a clock synchronous with the signal transmitted and at the same rate. By controlling the static phase of the clock the timing

of the decision point in the received data bit stream can be determined. In order to determined the jitter transfer function and the jitter generated by the receiver, the dynamic behavior of the phase and phase noise of the recovered clock needs to be controlled.

7. **Latch** - The latch retimes the quantized signal with the recovered clock to create an optimized signal with minimum amplitude and phase distortion.

The overall optical to electrical transfer function is tightly controlled so that the Inter-Symbol Interference and the signal-ASE beat noise is minimized.

The electrical signal from a TIA is fed to a high-gain limiting amplifier (GaAs MESFET) whose decision threshold is optimized automatically through a feedback circuit. Normally the decision threshold is slightly shifted toward "0" because signal ASE beat noise is much stronger in "1" than "0". The clean differential data outputs are then regenerated by a GaAs decision circuit and a Phase-Frequency Locked Loop (PFLL) retiming circuit.

The typical sensitivity of an optical receiver is -33dBm at the Bit Error Rate (BER) of 1.0x10^-10. In an optically amplified system as the DWDM system the ultimate performance can be only stated with the measured BER of the system. The BER performance can be indirectly estimated with measured OSNR of each channel which is the ratio of the signal power and the amplified spontaneous emission (ASE) noise normalized in certain optical bandwidth

and is easy to measure with an optical spectrum analyzer. The relationship between BER and OSNR is as follows:

$$BER = \frac{1}{4} erfc\left[\frac{\sqrt{2}(1-r)(\tau - c_{isi}^{-})Is}{(1+r)\sigma_0}\right] + \frac{1}{4} erfc\left[\frac{\sqrt{2}(1-r)(1-c_{isi}^{+}-\tau)Is}{(1+r)\sigma_1}\right]$$

where σ_0 and σ_1, the standard deviations of the total noise for marks and spaces, are functions of OSNR and other optical and electrical parameters such as: τ the actual decision threshold with respect to the spaces, c the percentage positive and negative eye closure, r the extinction ratio of the transmitter and Is the signal photocurrent. The complimentary error function, erfc (x) is defined as:

$$erfc(x) = \frac{2}{\sqrt{\pi}} \int_{x}^{\infty} e^{-x^2} dx$$

2.3.4 DWDM Filter Components

The WDM filter is a component used to demultiplex the multiplexed signal into its individual channels. The key characteristics of these filters are: The filter bandshape, rejection of the outband channels (crosstalk), and the optical insertion loss. The desired filter bandshape is a

rectangular shape with enough bandwidth to accommodate long term drift of the signal and filter wavelengths. There are two major technologies currently used by DWDM systems, the interferometric thin film filters and the waveguide-type devices. The latter filters are based on arrayed gratings fabricated with silica-based optical waveguides on a silicon substrate.

The interferometric thin film filter has an alternating array of thin films with high and low refractive indexes. Each film has an approximate thickness of a ¼ or ½ wavelength. The parameters of most importance are passband loss, passband width, and rejection band attenuation. Typically, the passband loss must be low, passband width must be wide, and rejection band attenuation must be large (more than 20-30 dB). The filter bandshape is determined by the number of cavities in the filter, for instance, a three cavity filter show an almost perfect square top and narrow skirts. Wavelengths deviations due to temperature changes can create interchannel crosstalk, and when the bandwidth of the bandpass filter decreases, crosstalk is less likely to occur but multiplexer loss increases. Interferometric thin film filters are currently available with the following characteristics: passband loss less than 0.2 dB, rejection band attenuation ranges from 25 to 30 dB, insertion loss from 1 to 5 dB, and crosstalk attenuation from 20 to 70 dB.

The waveguide-type filters have the advantages of planar technology which are: manufacturability, easy incorporation of complex optical circuits, and fiber connectivity. Some

waveguide-type WDM filters use a Mach-Zehnder interferometer, and the wavelength response is determined basically by the length difference ΔL, and not by the wavelength dependence on the directional couplers used in the Mach-Zehnder.

As illustrated in figure 2.5 [17].The fundamental layout of the waveguide-type filter consists of single-mode channel waveguides of different lengths and bent sections of the same curvature radius. Length difference between adjacent channel waveguides is given by $\Delta L = 2$ (D - d). Any two adjacent waveguides have the same length difference ΔL which results in a phase difference $2\pi n_c \Delta L / \lambda$, where n_c is the effective refractive index of the channel waveguide and λ is the light wavelength. The light exiting from the waveguide is diffracted at an angle θ which satisfies the equation

$$n_c \Delta L + n_s d \sin\theta = m\lambda$$

where n_s is the refractive index of converging space, d is the pitch of the channel waveguides at their exits, and m is the diffraction order. A waveguide-type filter with large ΔL can multiplex and demultiplex signals with small wavelength spacing, and the filter's ΔL can be designed to satisfy the desired wavelength resolution.

INTEGRATED NxN MULTIPLEXER

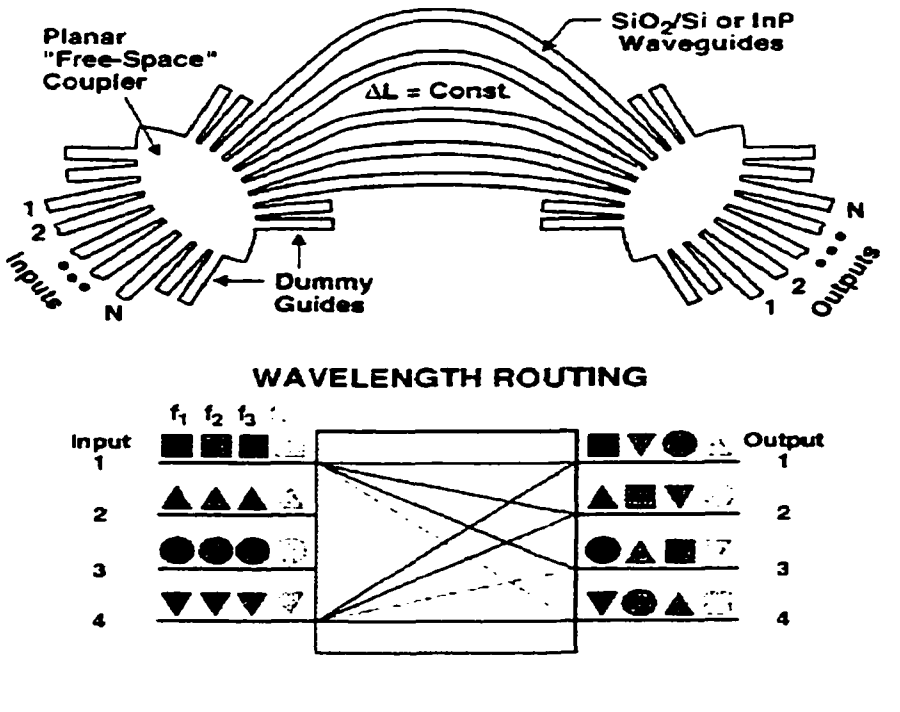

Figure 2.5. Optical Multiplexer/Demultiplexer Waveguide Filter

CHAPTER 3

Development and Characterization of the Two Key Enabling Technologies

3.1 Introduction

In this Chapter, we will develop novel wideband high output power EDFA configurations. The performance of these configurations will then be experimentally examined and analyzed. Furthermore, we will also characterize the performance of MUX/DMUX that are compatible with the proposed channel spacing of 50 and 100 Ghz.

3.2 *Novel Wideband High Output Power EDFA Configurations*

3.2.1 Fundamentals of Optical Amplifiers

An EDFA is a length of Erbium doped single mode fiber pump from its ends with diode laser sources (see figure 3.1). The pump power is coupled either into the input of the Erbium fiber (forward pumping), or into the output (backward pumping), or into both ends simultaneously (bidirectional pumping).

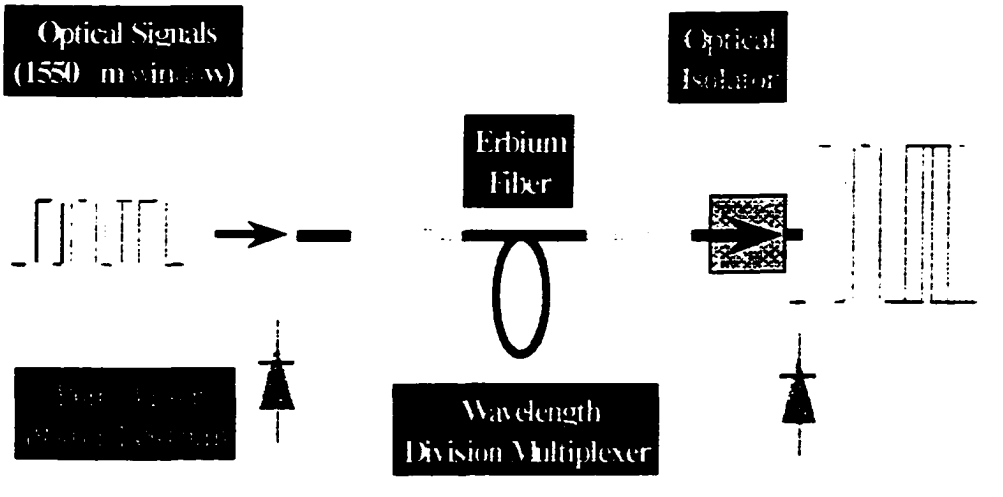

Figure 3.1. EDFA Bidirectional Pumping Configuration

The amplification effect is based on electron transitions between certain atomic levels of Erbium. Energy from incident pump photons elevate these electrons from a ground state to a

higher energy level, if the photon energy is just equal to the energy difference between these two levels. Excited electrons relax spontaneously or stimulated. Spontaneous decays are either nonradiative creating phonons, or radiative emitting photons with statistical phase and polarization. The density of excited states decreases exponentially with a time constant known as spontaneous lifetime. The stimulated decays are triggered by photons, whose energy agrees with the energy gap between ground and excited state. The emitted photons have the same phase and polarization as the stimulating photons (see figure 3.2).

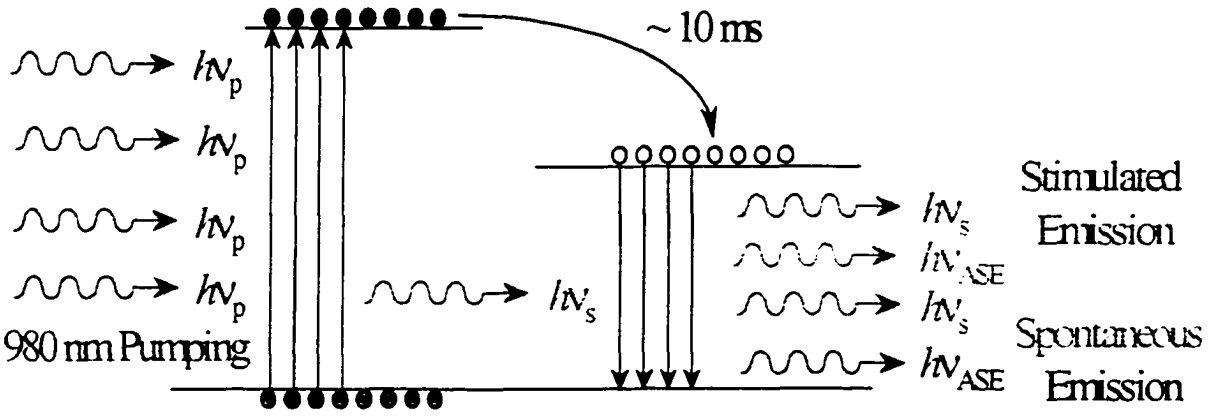

Figure 3.2. Energy Level Diagram for a Three Level System

With these considerations, an EDFA can be described as follows. Pump light propagating along the fiber is absorbed by ground state Erbium atoms lifting them to a higher state, the pump level. From there they decay very fast and nonradiatively to an excited level lying above

the ground state, but below the pump level. Since the spontaneous lifetime there of about 10 ms is relatively long, a population inversion between ground and excited level is established. That means, more or less of the Erbium atoms are in the excited state and the rest in the ground state. One part of the excited atoms is stimulated by photons of an incident signal to emit additional photons, if their wavelengths correspond to the energy gap between ground and excited level, thus amplifying the signal. The other part decays spontaneously. The spontaneous emission propagates towards both ends of the Erbium fiber, i.e. in forward and backward direction, and is amplified concurrently with the signal. This generates optical spectra, known as forward and backward Amplified Spontaneous Emission (ASE). The forward ASE degrades the signal to noise ratio on the detector diode.

The Erbium atoms in the ground state reabsorb signal and ASE, since they can be lifted directly to the excited state by photons with signal wavelength. Therefore, a signal propagating along the fiber will increase as long as this absorption is dominated by stimulated emission, i.e. the pump power remains beyond a certain threshold value. Due to the pump absorption, the pump signal can get below this threshold, if the fiber is too long. The EDFA has thus a maximum gain for a defined fiber length.

3.2.2 Comparison of Experiment and Simulation of Optical Amplifiers

3.2.2.1 Introduction

The design of novel OA configurations requires the use of new and improved Er-doped fibers. The Erbium fiber used in this experiment is designed to maximize gain and output power as well. For the design of the OA itself and system simulations a simulation tool is necessary which can model both the OA and the performance of other parts of the transmission link, i.e. the fiber, transmitter and receiver. The simulation tool used has this capability but the Erbium fiber parameters for the fiber utilized in the experiment were not available, yet.

Therefore, we built a single and double stage OA configuration and we measured and simulated the gain flatness of both configurations. The simulation parameters for the Erbium fiber were fitted in such way that a good agreement with the measurement results could be achieved.

3.2.2.2 Experimental Setup

The gain flatness was measured with an electrical method. A low power probe signal (-30dBm) scans the interesting wavelength range while the OA is saturated by another saturating signal at 1555 nm. This signal is located in the middle of the transmission band from

1548.5. 1560.6 nm (16 channel application). The probe and the saturating signal are combined by a 3 dB-coupler. This measurement setup makes a gain flatness measurement over a wide wavelength range possible without requiring a large number of probe signals.

The scanning signal is modulated with a 300 kHz tone. After calibrating the setup with shorted fiber the OA is spliced within the configuration and measured. The power of the modulation is measured with an electrical spectrum analyzer (ESA) after O/E conversion. The electrical method gives two advantages compared with the direct optical spectrum analyzer (OSA) measurement:

- The O E conversion of the ESA is polarization independent.
- Any ASE power has a white noise spectrum in the base band with low power at each frequency and does not effect the 300 kHz tone.
- The modulated probe signal is not influenced by the unmodulated saturating signal, which has much higher power, even if the wavelength is near by or the same.

The power of the saturating signal is controlled by an additional tap coupler (10 dB) in front of the OA input (see figure 3.3).

3.2.2.3 Optimization Procedure

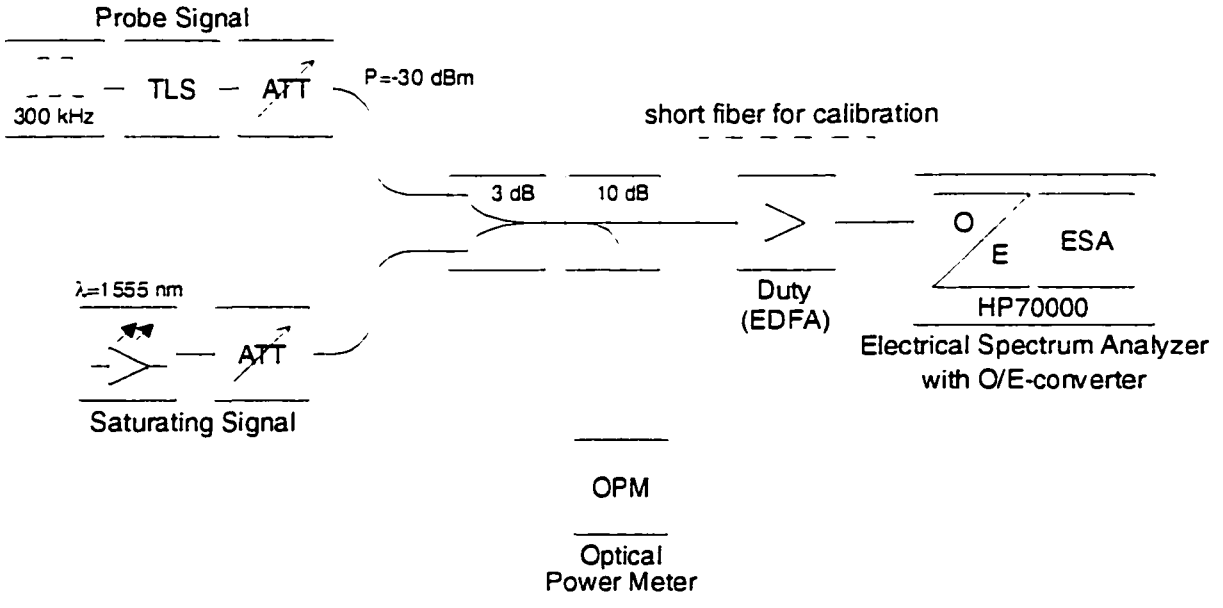

Figure 3.3. Measurement Setup for Gain Flatness Measurement

First, the gain flatness was measured for a forward pumped single stage OA in order to make the configuration for measurement and simulation as simple as possible. Therefore the number of components and splices is small and discrepancies, i.e. for insertion losses, between measurement and simulation will also be small.

The single stage OA was measured with 3 lengths (12m, 16m, 20m) and different input powers, i.e. saturating powers, and pump powers. Then, the same configuration was simulated

and the simulation fiber parameters, which were first extracted from the Giles-parameters, were fitted. Two parameters were changed:

- The dopant concentration was decreased from $4.29*10^{24}$ to $3.75*10^{24}$.
- The pump efficiency was increased from 85% to 90%.

With these changes the simulation results were very close to the measurement results for different fiber lengths and different operating conditions (see section 3.2.2.4). Finally, a double stage amplifier was simulated and designed with the optimized fiber parameters. The first configuration was built with 12m and 16m Erbium fiber for the first and the second stage, respectively. The measurement and simulation results are given in section 3.2.2.5.

3.2.2.4 Measurement and Simulation of Single-Stage OA

The single stage OA was a forward pumped configuration. The pump power was measured behind the WDM in order to get the most accurate value by taking into account the WDM and the splice between pump laser and WDM. A Corning Flexcore pigtail with angled connector was spliced at the output of the WDM to reduce splice loss during the power measurement and reflections which could influence the spectral behavior of the pump laser module. The insertion loss of the passive optical components was also measured. The values of the components and additional attenuation for the splices are given in figure 3.4.

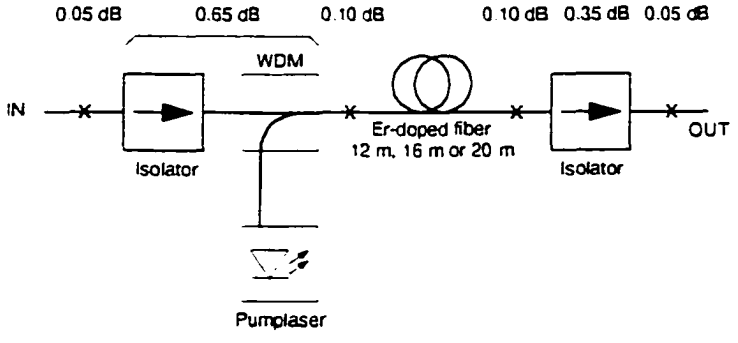

Figure 3.4. Configuration of Single-Stage OA

The configurations for the corresponding simulation EDFA-model is given in figure 3.5. There is no additional loss in the pump path because the pump power was measured behind the WDM. The splice loss between WDM and Er-doped fiber is assumed to be the same as the splice loss to the Corning Flexcore fiber during pump power measurements.

The measurement and simulation results are shown in Figure 3.6 to Figure 3.9. They are displayed for 12 m and 20 m fiber length for different input powers, i.e. saturating powers and pump powers. The wavelength range is on one hand the whole measurement range from 1525 nm up to 1565 nm and on the other hand s from 1548 nm to 1562 nm close to the operating window for 16 channels with increased resolution.

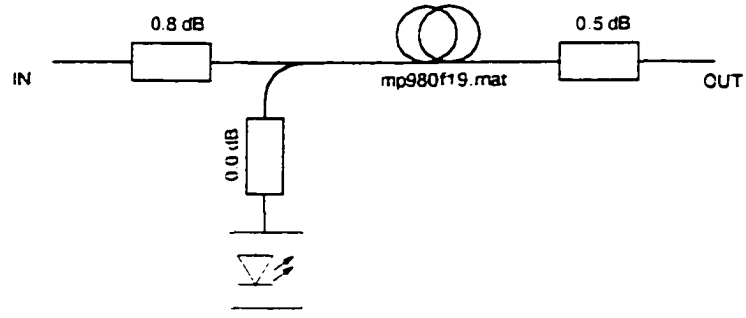

Figure 3.5. Parameters in Simulation of EDFA-Model for Single-Stage OA

The simulation results are very close to the measurement results even under very different conditions, i.e. fiber length, input and pump power. In the WDM window the simulation results are slightly higher than the measurements. The differences near the gain peak are a bit more significant. Discrepancies in the simulation parameters leads to a larger mistake due to higher emission and absorption values in that area.

With these first results for a single stage OA the simulation for a double stage OA is expected to be also accurate.

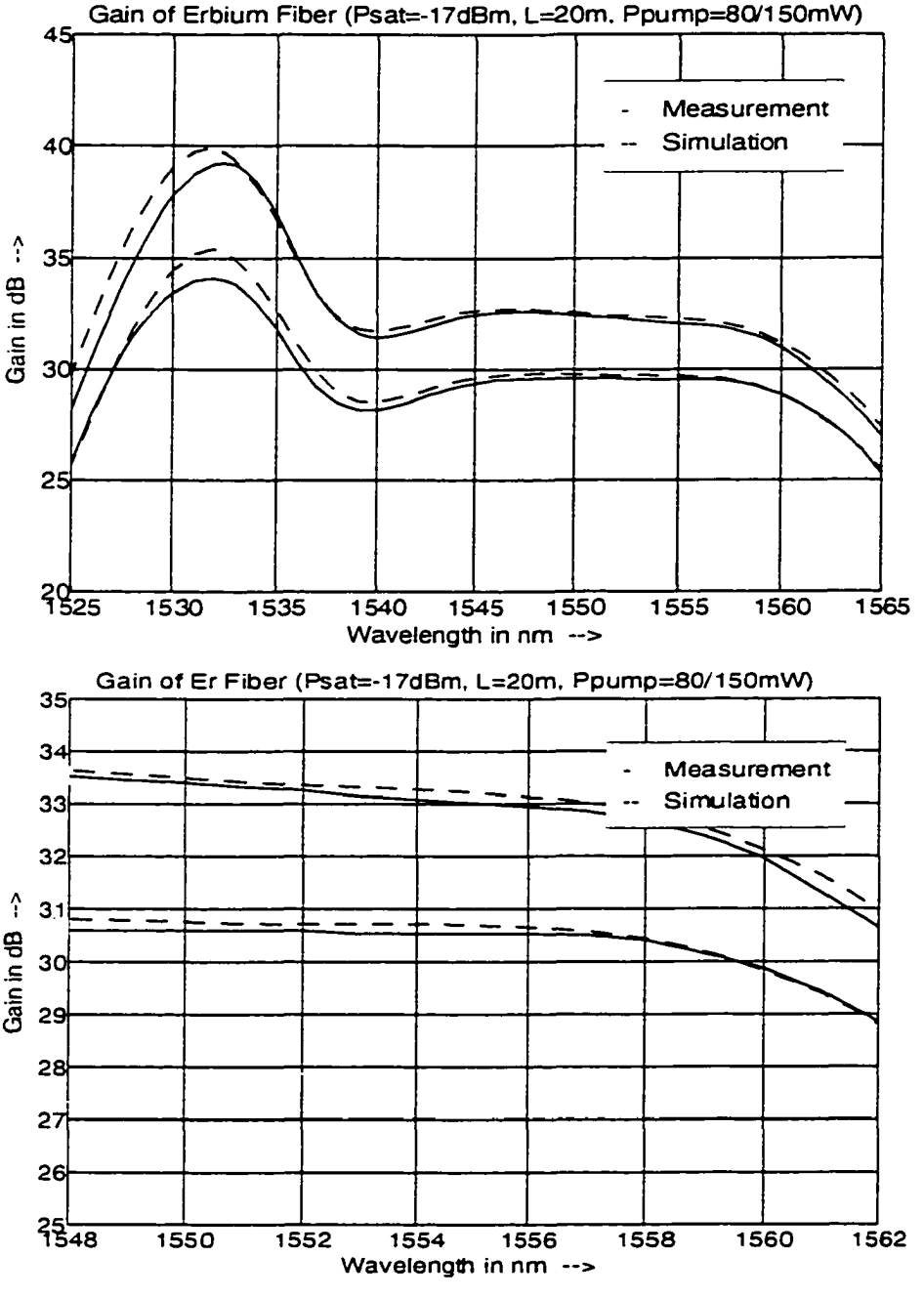

Figure 3.6. Gain of Single-Stage OA with 20m Er Fiber and P_{in}= -17dBm

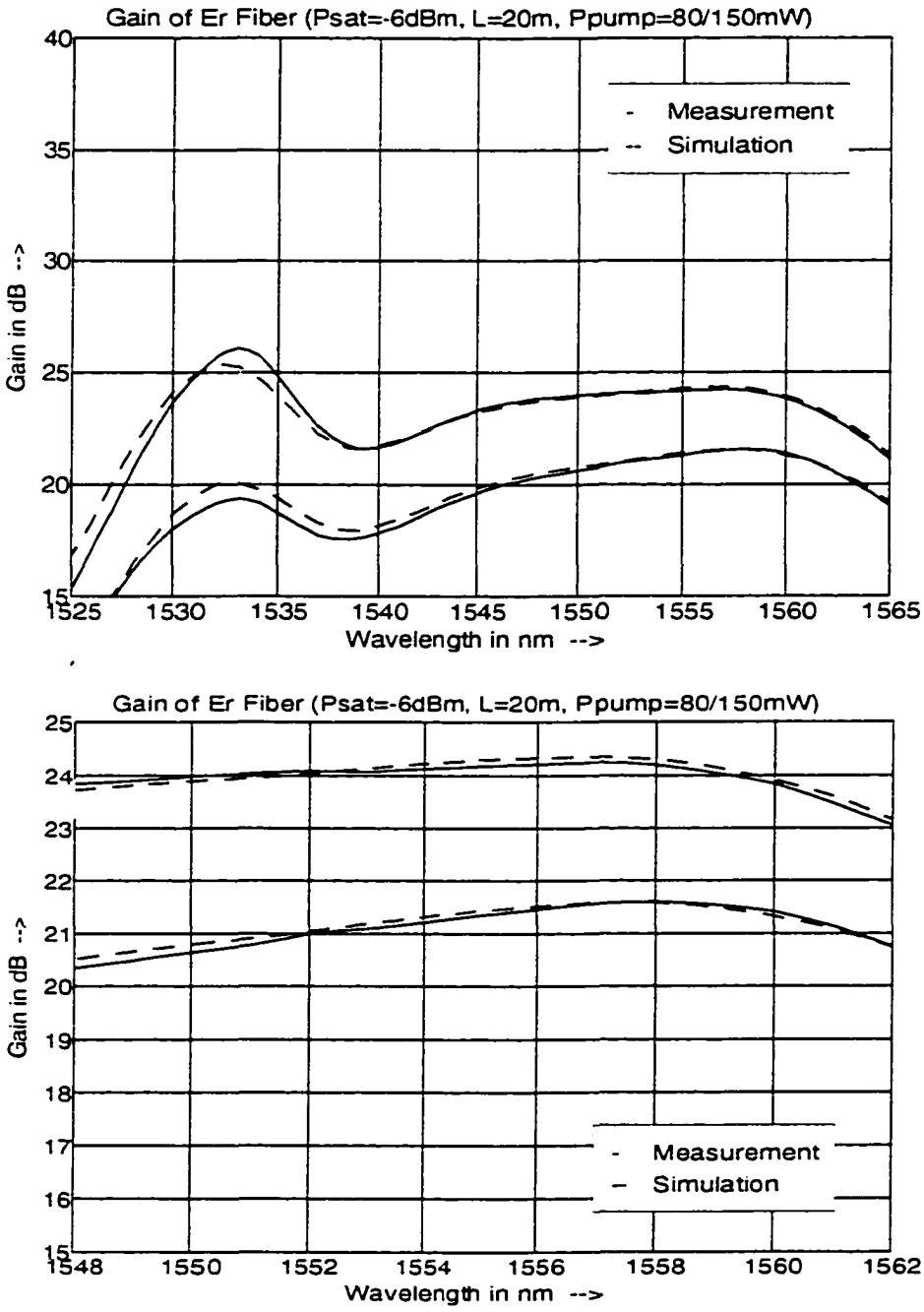

Figure 3.7. Gain of Single-Stage OA with 20m Er Fiber and P_{in}= -6dBm

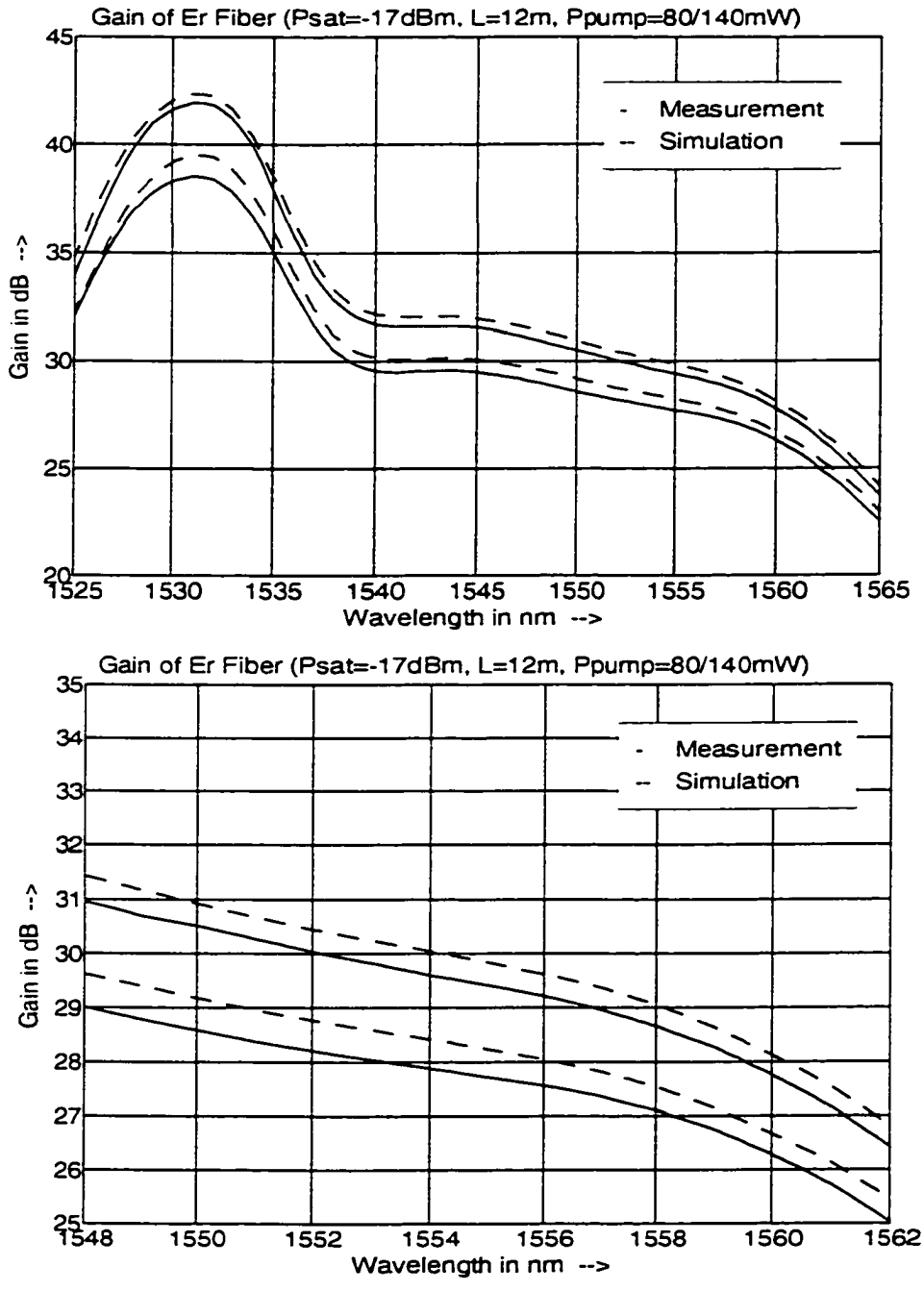

Figure 3.8. Gain of Single-Stage OA with 12m Er Fiber and P_{in}= -17dBm

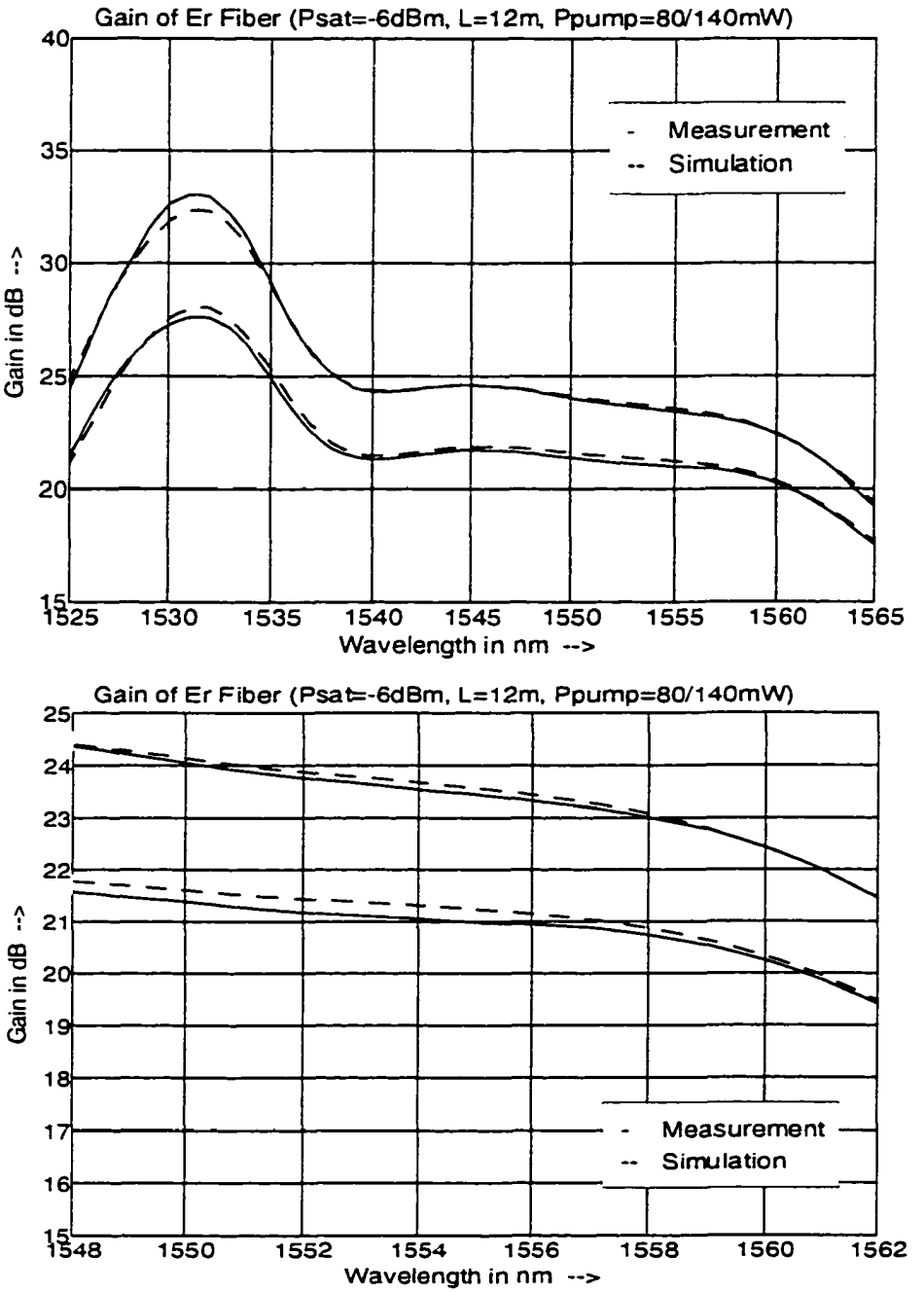

Figure 3.9. Gain of Single-Stage OA with 12m Er Fiber and P_{in}= -6dBm

3.2.2.5 Measurement and Simulation of Double-Stage OA

The double stage OA has a backward pumped first stage and a forward pumped second stage. The configurations of both the OA and the simulation EDFA-model are shown in figures 3.10 and 3.11. Until now, just one configuration with 12 m Erbium fiber for the first and 16 m for the second stage was built up, measured and simulated.

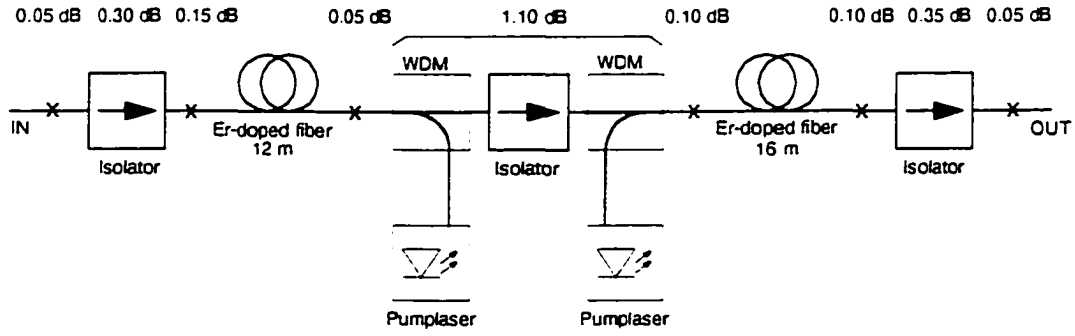

Figure 3.10. Configuration of Double-Stage OA

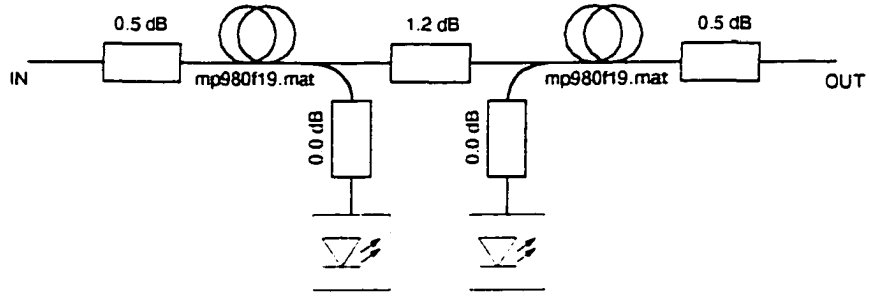

Figure 3.11. Parameters in Simulation of EDFA-Model for Double-Stage OA

The measurement and simulation results are shown in Figure 3.12 and Figure 3.13. They are printed for a pump power of 80 mW and 140 mW into both stages, respectively. The saturating powers are -17 dBm and -6 dBm. Again, the wavelength range is on one hand the whole measurement range from 1525 nm up to 1565 nm and on the other hand from 1548 nm to 1562 nm close to the operating window for 16 channels.

The simulation results for the double stage OA are also very close to the measurement results. For small input powers, i.e. -17 dBm, the agreement is good over the whole wavelength range. For higher input powers, i.e. -6 dBm, there is a small difference near the gain peak.

3.2.2.6 Conclusion

After fitting the simulation parameters the simulation results are very close to the measurement results. Both a single and a double stage OA could be simulated accurately. Especially, the agreement in the 16 channels WDM window is excellent. There, the difference is smaller than 0.5 dB. Near the gain peak at 1530 nm and under special conditions the differences between simulation and measurement are a slightly higher.

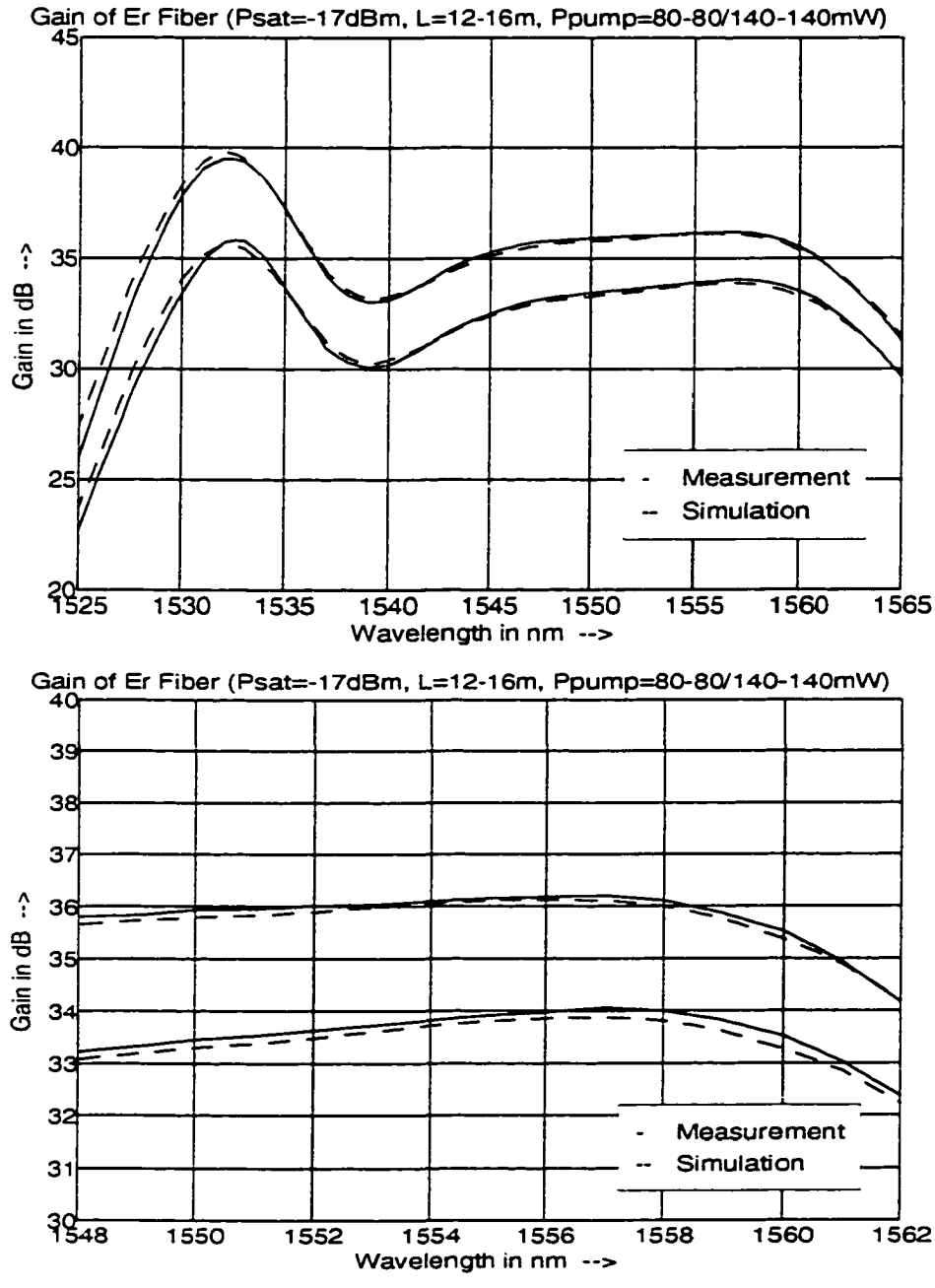

Figure 3.12. Gain of Double-Stage OA with 12/16m Er Fiber and P_{in}= -17dBm

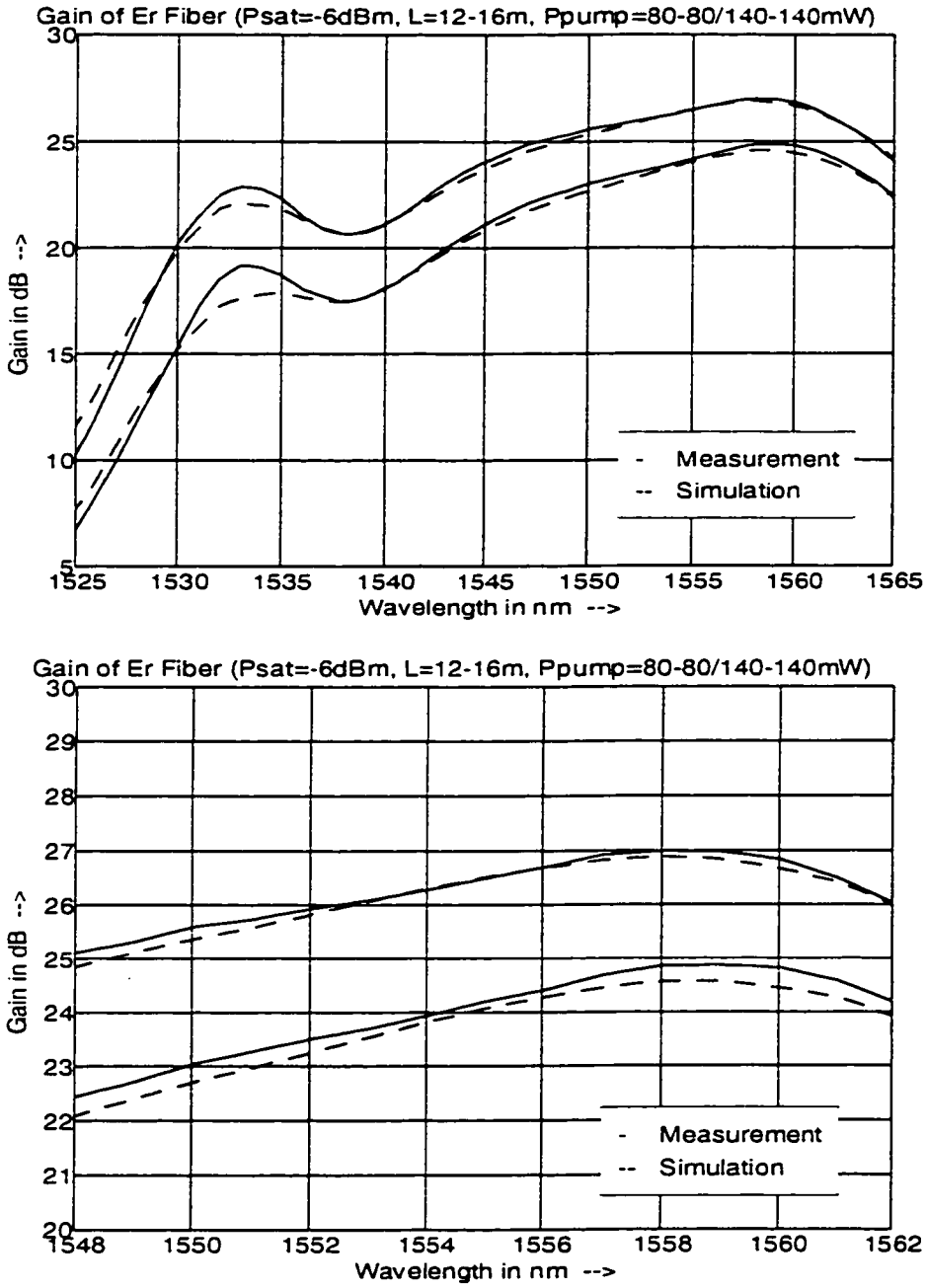

Figure 3.13. Gain of Double-Stage OA with 12/16m Er Fiber and P_{in}= -6dBm

3.3 *Mux/Dmux Compatible with 50/100 Ghz Channel Spacing*

3.3.1 Introduction

The two filtering technologies most widely used to produce narrowband or densely channel-spaced WDMs are planar phased-array waveguides (PAWs), and thin-film dielectric interference filters [1]. Between these two technologies, the PAW is the most available component with the flexibility of large channel number and narrow channel spacing. In the following sections we will analyze the PAW as the demultiplexer for our 16-channel/100Ghz channel spacing system, as well as for our 64/100 channel with 50 and 100 Ghz channel spacing. Furthermore, we will give a brief description of the thin-film dielectric interference filter technology.

3.3.2 Design Considerations of Large-Number and Narrow Channel Spacing DMUX

The systems to be described in chapters 4 and 5 will offer the capability of carrying 16, 64, and 100 wavelengths at 2.5 and 10 Gbit/s bit rates with 100, 50/100, and 50 Ghz channel spacing respectively. Many challenges are caused by the large number of channels at such narrow channel spacings. The two major problems we face with such dense systems are, wavelength stability for both transmitting lasers and demultiplexers due to the restricted channel space,

and the increased total crosstalk due to the large channel count. Let's discuss the topics of wavelength tolerance, wavelength detuning, crosstalk dependence on number of channels, and crosstalk degradation due to power divergence and wavelength shifting in the PAW filter technology.

3.3.2.1 Wavelength Tolerance

In the development of robust and reliable systems, time plays an important role in the design of each of its devices. Narrow channel spacing systems require very tight limitations on the demultiplexer parameters so that the system remains robust over long periods of time. This leads to specified wavelength accuracies for channel spacings as small as 50 Ghz. To insure acceptable adjacent crosstalk we need to have filters with full width at half maximum bandwidth (Δf_{3dB}) equal to half of the channel spacing, i.e. Δf_{3dB} = 25 Ghz. With less than 3dB power penalty, it is required that the filter has a total wavelength variation of +/- 12.5 Ghz. This means that the total tolerable wavelength excursion should be very tight. This tolerance should include shifting effects due to temperature, aging, polarization, and wavelength offsets. When this same filter technology is used for both 50 and 100 Ghz channel spacing systems, the 50 Ghz channel spacing system is strongly affected by the wavelength drift in much higher proportions than the 100 Ghz system.

3.3.2.2 Wavelength Detuning

The worst case scenario of wavelength detuning is shown in figure 3.14(a)(b). In addition to an approximately 3 dB power loss, the more serious effect is the adjacent crosstalk degradation in the 50 Ghz channel spaced demultiplexer. The impact of wavelength detuning depends greatly on the filter passband shape.

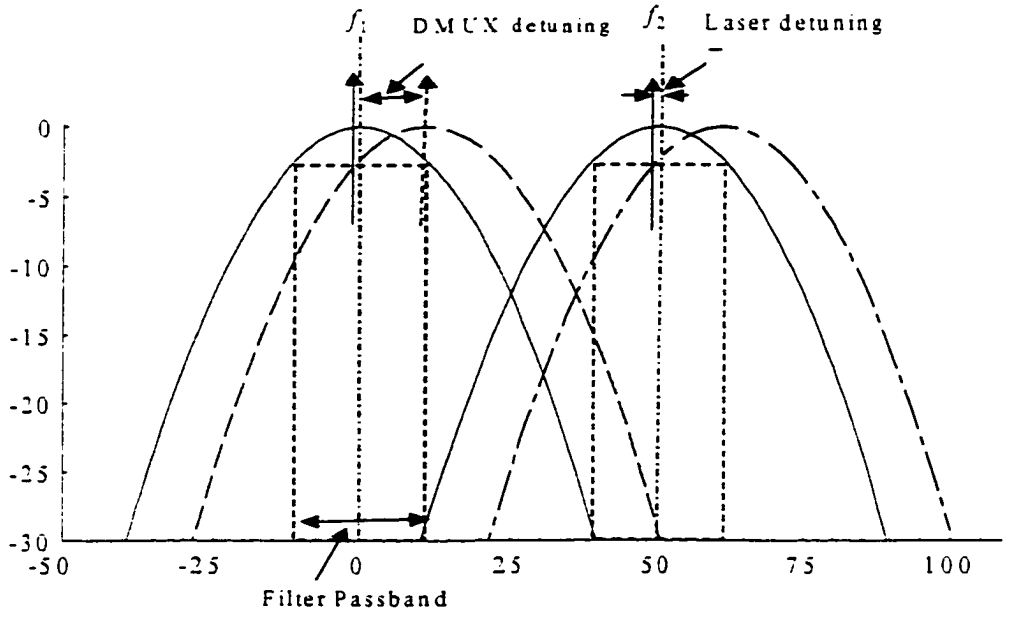

Figure 3.14(a). The worst case wavelength detuning between signal and DMUX for a peaked router.

In figure 3.14(a), the adjacent crosstalk degrades to about -14dBm in a gaussian peaked demultiplexer. In figure 3.14(b) the adjacent crosstalk rejection is better than 25 dB with the worst case detuning in a flat top demultiplexer. The major concern with the flat top DMUX is

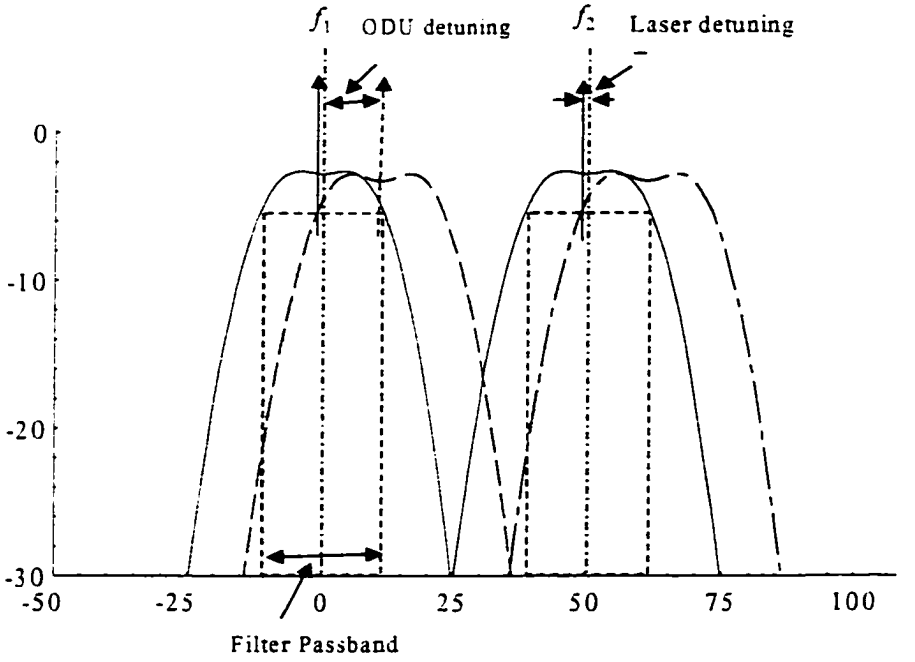

Figure 3.14(b). The worst case wavelength detuning between signal and DMUX for a flat-top router

the difficulty to control the filter-edge steepness during the fabrication. Therefore, it creates uncertainties with respect to the accuracy of the adjacent crosstalk rejection value. Compared to the flat top filter the peaked shaped router is relatively easier to fabricate.

Due to the technological challenges of the 50 Ghz channel spaced demultiplexer, it requires careful design and fabrication.

1. Adjacent crosstalk and system penalty degradations together with power loss due to wavelength drifts and offsets, will play a dominant role in the design of narrow channel spacing DWDM systems.

2. Channel spacing can not be tuned after fabrication.

3. A restrict wavelength tolerance limits the availability of the filters.

4. A filter with low crosstalk is limited by the phase error caused by fabrication non-uniformity of the device.

3.3.2.3 Optical Crosstalk in DWDM routers

In DWDM routers, the phase error associated with the larger chip size generates a degradation in the channel crosstalk of the demultiplexer. A 50 Ghz PAW router design requires a larger slab-coupler focal length or a smaller grating pitch (see figure 3.15). Resulting in a larger number of grating waveguides and a larger chip size compare to the 100 Ghz router. Theoretically, in an ideal router without any phase error, a technique to lower the crosstalk is to increase the number of grating waveguides. In the other hand, a fabricated router experiences phase error due to distorted power distribution in the grating waveguides and fabrication non-uniformity, degrading crosstalk performance. To counterattack the impediments mentioned above, improved fabrication using ultra-high resolution mask [2], post-fabrication crosstalk compensation, etc. schemes are needed.

3.3.2.4 Analysis of Total Crosstalk

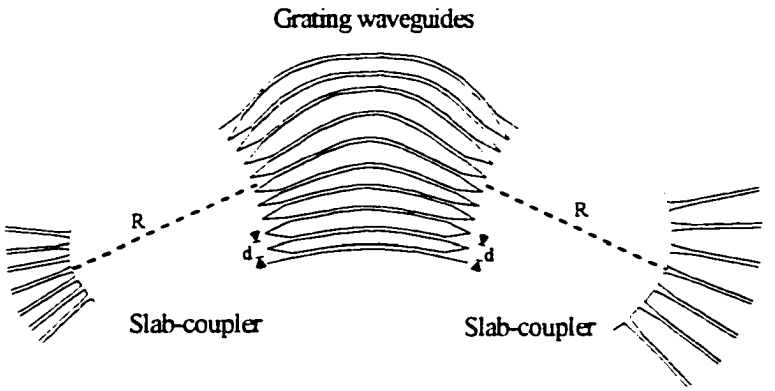

Figure 3.15. Schematic drawing of the PAW router. R = Slab-coupler focal length. d = Grating pitch

Total crosstalk caused system penalty can be estimated using the eye closure [3].Condiser-ing the channel power divergence (the power variation due to the spectral gain dependence in the optical line), the crosstalk at j-th channel C_j (dB) can be obtained by summing the total power leaking through the demultiplexer from all possible channels in the system, given by

$$C_j = \sum_{i=j\pm 1} 10^{C_{j,j\pm 1}/10} \cdot 10^{(P_i - P_j)/10} + \sum_{i\neq j, j\pm 1}^{N} 10^{(P_i - P_j)/10} \cdot 10^{C_{j,i}/10}$$

Where C_{jj+-1} is the adjacent crosstalk level in dB at j+/-1 -th channels of the j-th channel spectrum, $C_{j,i}$ is non-adjacent crosstalk level in dB at the window of the i-th wavelength of the j-th channel spectrum, and P_i is power level in dB at i-th channel before entering the demulti-

plexer. The channel crosstalk can be classified into two types: adjacent crosstalk (mainly caused by the filter passband shape) and the non-adjacent crosstalk (caused by phase error). Theoretically, a gaussian peaked filter with 50 Ghz channel spacing gives better than -25 dB adjacent crosstalk, as shown in figure 3.14(a).

3.3.2.5 Total Crosstalk Dependence on Channel Count

The impact of crosstalk is greater for systems with a large channel count. For large-scale demultiplexers, non-adjacent crosstalk from all other channels dominates, while the adjacent crosstalk only contributes a small percentage of the total crosstalk. Channel crosstalk limits the number of allowed channels in the DWDM system. Assuming a total crosstalk limit of $C_{allowable}$, the maximum number of channels is estimated by

$$N < 10^{(C_{allowable} - C_{non-adj})/10} - (2 \cdot 10^{(C_{adj} - C_{non-adj})/10} + 3)$$

where $C_{non\text{-}adj}$ and C_{adj} are the worst case of all non-adjacent crosstalk and adjacent crosstalk values. Assuming and allowable total crosstalk of -15 dB, the demultiplexer crosstalk level must be less than -30 dB for 64 channels. This number is valid assuming channel power equalization in the optical line and a perfect wavelength alignment between transmitting lasers and PAW router.

3.3.2.6 Total Crosstalk Degradation by Channel Power Divergence

The effect of crosstalk depends on the amplitude and shape of the channel power divergence.Therefore, it is imperative to design the in-line amplifiers as to give minimum gain variation and power divergence. Equalization schemes are necessary to improve the channel power variation in systems with a large number of concatenated amplifiers. The equalization scheme is explained in detail in section 3.2.3. Power divergence can also be caused by the variable outside plant loss of the link. In the system evaluated in the following chapters all outside plant losses are assumed fixed to simplify the design of the optical amplifiers.

3.3.3 Thin-Film Filter Technology

Optical interference filters are relatively easy to manufacture in quantity, offer good optical performance, and are easily packaged into fiberoptic devices [1]. However, these filters suffer from poor temperature stability, and have not been able to reproduce narrow channel spacing demultiplexers for DWDM systems.

The Multilayer Interference filters (MI), are built from thin film structures by alternating layers of high and low refractive index [4]. Each layer has a thickness equal to one half or quarter wavelength (1500 nm). Figure 3.16 shows the structure of such thin film cavity, where the number of alternating layers could vary from 20 to 30 layers. Placing these thin film filters on a rectangular glass substrate, and employing multireflection, multiplexing can be achieved.

As shown in figure 3.16, one particular wavelength will pass through one filter and the rest will be reflected. The reflected beam will go through the same cycle of transmission and reflection at the opposite filter in the rectangular structure.

The advantage of MI over PAW filter types is that it does not require temperature control, which makes them simpler to use. Another advantage is the relatively lower insertion loss and

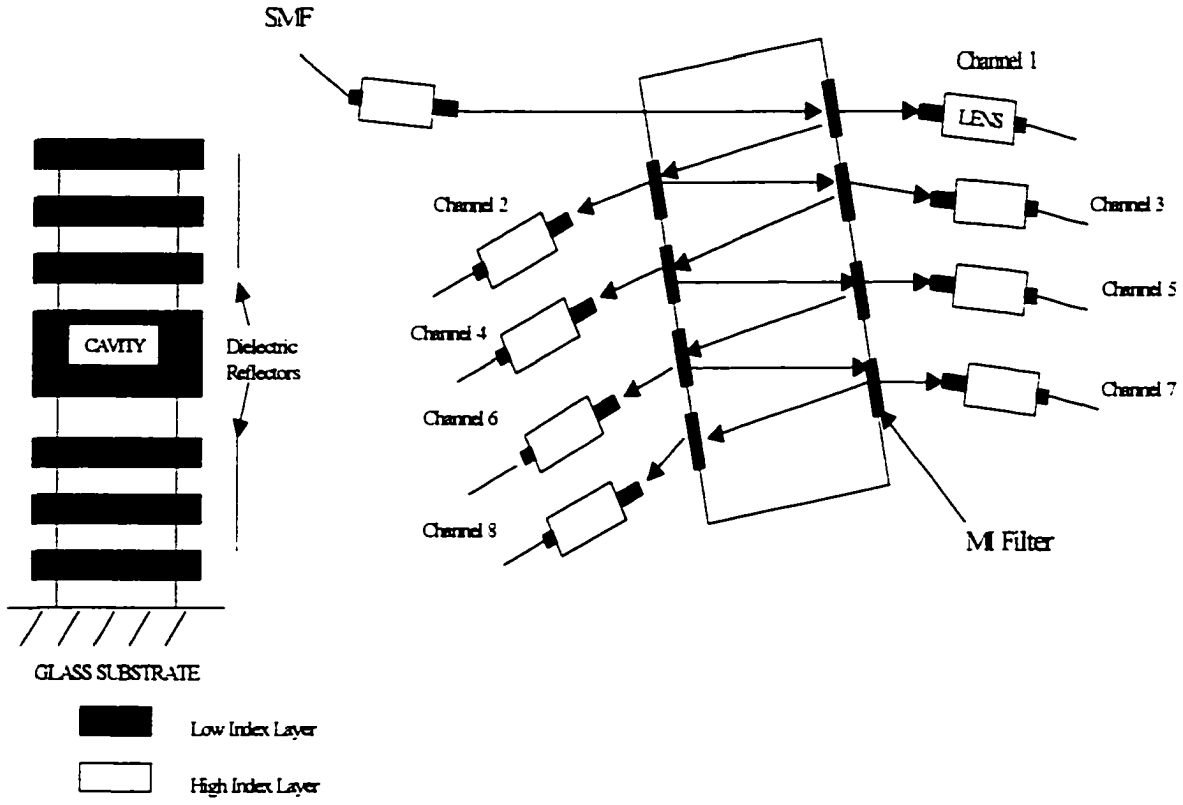

Figure 3.16. Structure of a multilayer interference cavity thin film based multiplexer [5].

better crosstalk performance. In addition, a pair MUX/DMUX can be designed and combined to give a flatter and lower insertion loss compared to the PAW.

3.3.4 Fiber Grating Technology

The fiber bragg gratings are created directly in the GeO_2-doped core of optical fibers. The UV light is absorbed by the germanium defects in the core, and as a result there is a variation in the periodic index of refraction creating a bragg reflector (see figure 3.17). The bragg wavelength, λ_B, is given by

$$\lambda_B = 2\Lambda n_{eff} = \lambda_{UV}/(2\sin\alpha)$$

where Λ is the period of the index of refraction variation and α is the angle between the interfering UV beams [6]. The bragg wavelength is determined to within a fraction of an angstrom by α and λ_{UV}. The index change remains after the UV light is removed. Figure 3.18 shows a typical transmission and reflection spectra of a fiber bragg grating. The transmission spectra shows 100% transmission of the light except at the bragg wavelength. On the other hand, the reflection spectra shows that the light at the bragg wavelength is reflected back to the fiber and generally an isolator is placed to eliminate this reflected light.

3.3.4.1 Fiber Bragg Grating Applications

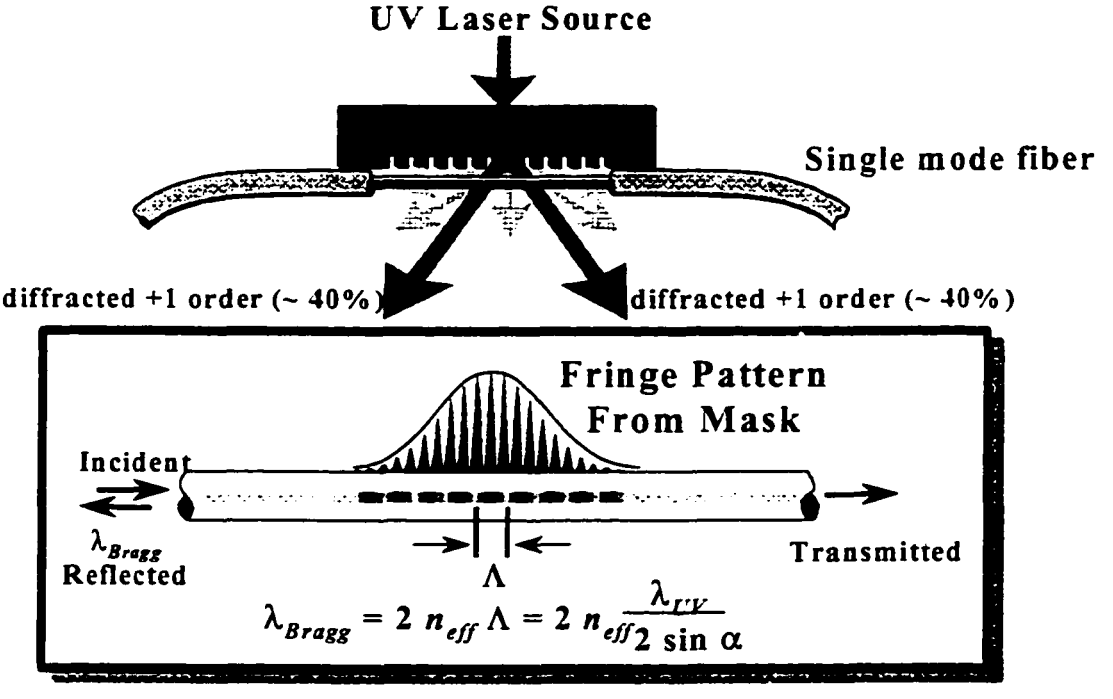

Figure 3.17. Writting a fiber bragg grating

Fiber bragg gratings can be used in a number of different applications (figure 3.19), fiber lasers, laser wavelength stabilization, pump reflectors, filters, demultiplexers, dispersion compensators, and gain equalization.

In DWDM systems, is imperative to flatten the EDFA gain spectra in order to increase the usable bandwidth. One approach to solve this problem is by using long-period fiber gratings. These are gratings with periods in the order of tens of micrometers. Unlike fiber bragg gratings that reflect light back down the fiber, long-period fiber gratings scatter light forward into

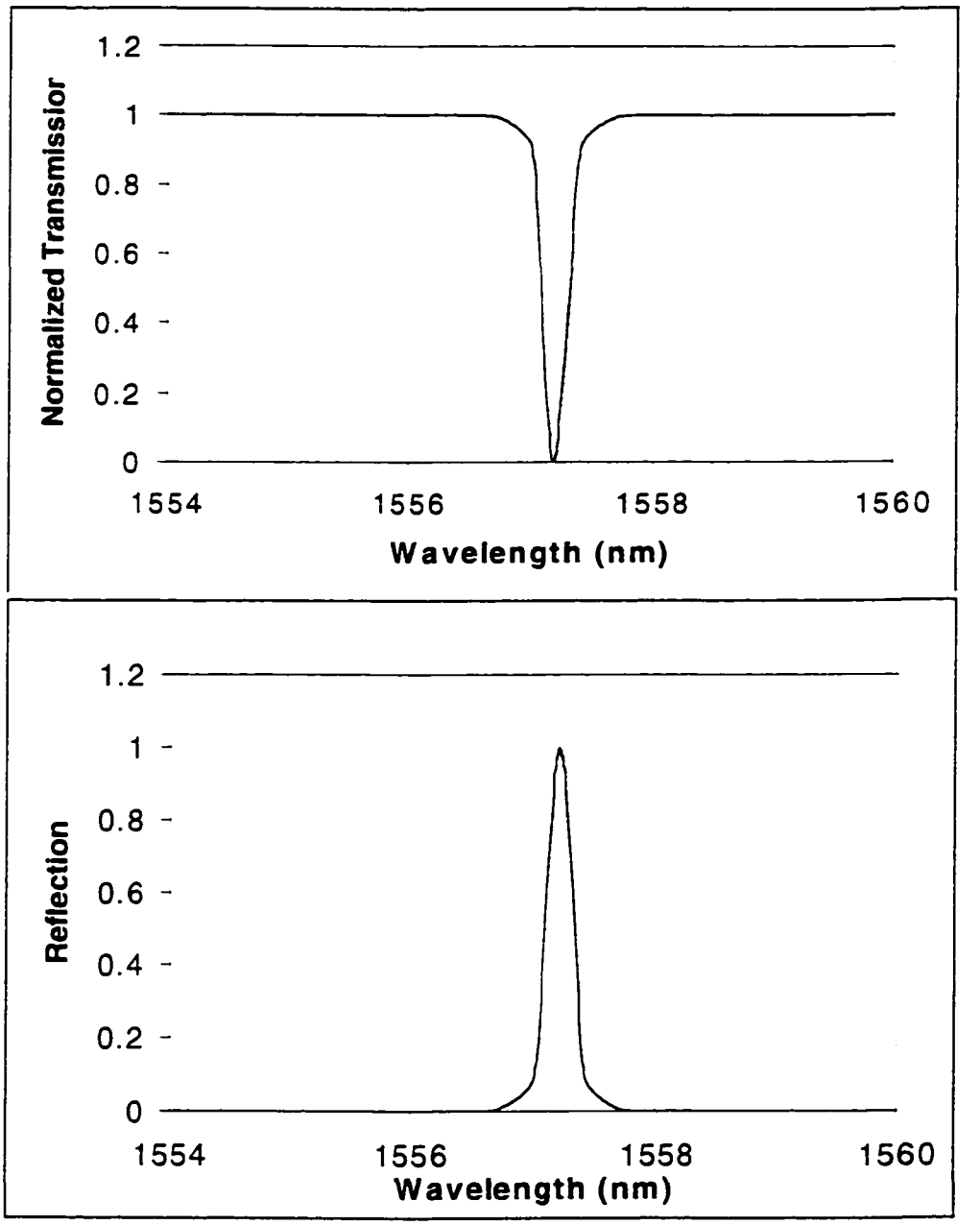

Figure 3.18 (a) Transmission and (b) reflection spectra of a fiber bragg grating.

cladding or radiation modes, where it is lost. This results in extremely low back reflections of approximately -80dB. The most important feature of the long-period gratings, is that it can be tailored to closely resemble the inverse of the EDFA gain spectrum. As a result, the output of a fiber amplifier can be flattened as to be able to concatenate a large number of amplifiers with minimum gain variation.

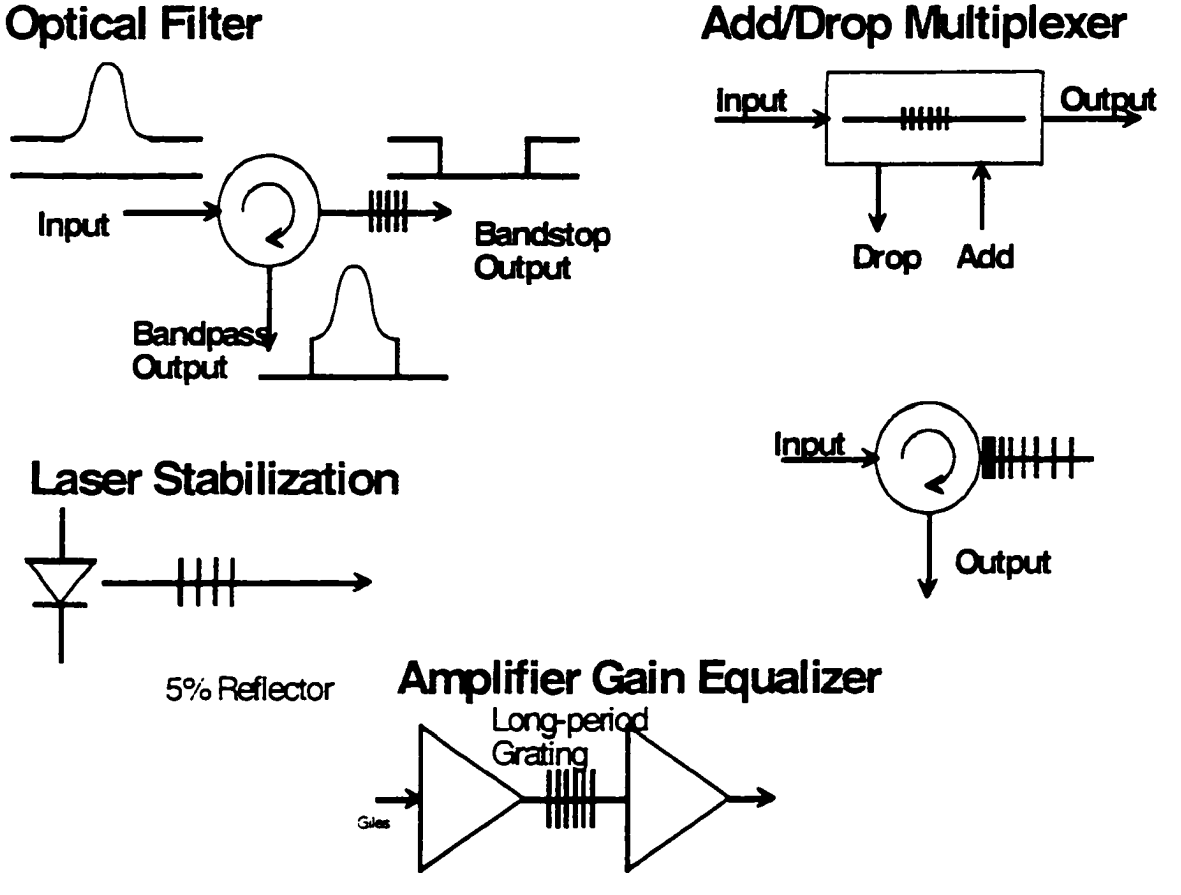

Figure 3.19 Applications of fiber gratings.

CHAPTER 4

16 x 2.5 Gbit/s DWDM Transmission System Demonstration

4.1 Introduction

DWDM transmission systems are now being deployed on a very large scale in commercial networks. The transmission of these long-haul DWDM systems can be limited by the finite bandwidth of the silica-based Erbium-Doped Fiber Amplifier (EDFA) repeaters and the non-linear interactions between channels. To further increase capacity with a channel spacing compatible with practical filtering technology, as well as to increase wavelength routing network capability, the number of channels must grow. Capacity of thirty two 10 Gb/s channels transmitted 640 km [1] and thirty two 5 Gb/s channels transmitted 9300 km [2] have been demonstrated in system experiments using silica-based EDFA repeaters.

In the following sections, we demonstrate transmission of sixteen 2.5 Gb/s WDM channels with 100 GHz spacing over 800 km of standard single mode fiber (SMF) using silica-based EDFAs. Standard SMF was chosen as most of the existing optical networks are based on this type of fiber. In addition, standard SMF is virtually unaffected by nonlinear interactions between channels due to its high dispersion. Since the number of transmitter lasers were limited, we could only performed experiments with 16 wavelengths. Simulations were also performed on the same system configuration in order to obtain a simulation result that will match the experimental measurements. Again, SMF was used in the simulations and nonlinear effects were not taken into account throughout the simulations.

4.2 Experimental Results

Figure 4.1 shows the experimental setup of the 16 x 2.5 Gbit's transmission system. The optical signals of 16 External Modulated Lasers (DFB laser plus an Electro Absorptive Modulator) were multiplexed into a Single Mode Fiber using a 16 channel combiner centered around 1555 nm, with approximately 0.8 nm spacings. The DWDM system consists of sixteen WDM channels spaced 0.8-nm apart in the 1548.5 (channel 1) to 1560.6-nm (channel 16) amplifier band. The silica-based EDF used is a commercially available amplifier. The EDFA configuration used in the measurements consists of a dual-stage EDFA, counter-pumped with

90 mW of pump power at 980-nm in stage 1 and copumped with 90 mW at 980-nm in stage 2. Both stages were optimized for gain flatness over the signals bandwidth. The noise figure (NF) is calculated to be below 4.4 dB for all wavelengths across the WDM signals bandwidth.

The amplifier chain consists of 9 dual-stage silica-based EDFAs. The input signal levels to the cascade of EDFAs are -25 dBm. channel at the input of the first amplifier.The transmission fiber consisted of eight 100 km spans of standard SMF having an average chromatic dispersion of + 16 ps/km-nm and an average attenuation of 0.25 dB km, for a total transmission distance of 800 km. The span loss between amplifiers is set equal to the average dual-stage amplifier gain of 25 dB. This corresponds to 100 km of fiber at 0.25 dB/km.

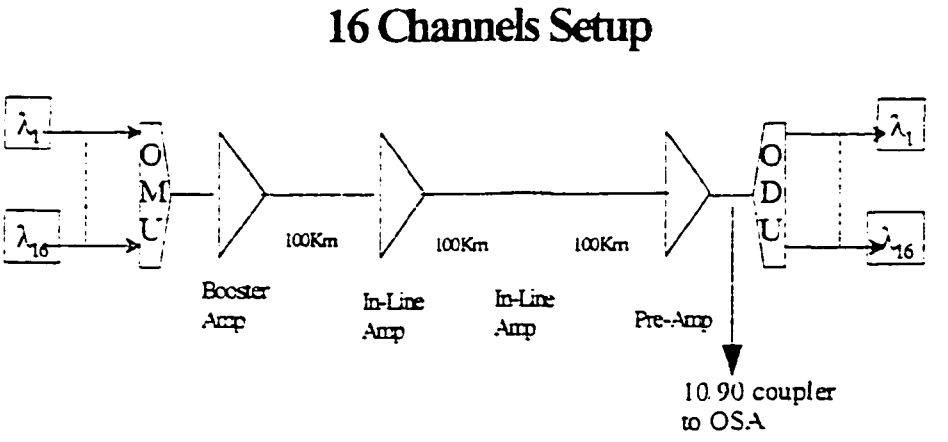

Figure 4.1. Experimental setup of 16 x 2.5 Gbit/s Transmission System

The signal and ASE power accumulation along the EDFA chain is measured at the output of the 9th Optical Amplifier (OA) with an OSA at 0.2 nm resolution bandwidth. The accumulated optical signal-to-noise ratio (SNR) reported here is the ratio between the signal level and the accumulated ASE noise power in a 0.2-nm optical bandwidth. The end-to-end system performance is estimated from the optical (SNR), which must be more than 18 dB (0.2 nm resolution) to achieve a bit-error ratio (BER) < 10^{-12} at 2.5 Gb s.

Figure 4.2 shows measurements of the signal levels and the accumulated ASE power (in a 0.2-nm optical bandwidth) immediately after the first and 9^{th} amplifier along the cascade. The SNR is greater than 33 dB after the first amplifier, and remains greater than 20 dB (0.2 nm resolution) for all channels after the 9^{th} amplifier. The output signal levels experience a power divergence of 5 dB at the end of the link, with approximately 3 dB SNR differential after the 9^{th} amplifier. The overall flatness at the end of the amplifier chain was obtained by using transmitter pre-emphasis (transmitter powers were manually chosen to achieve an optimized flatness at the end of the link).

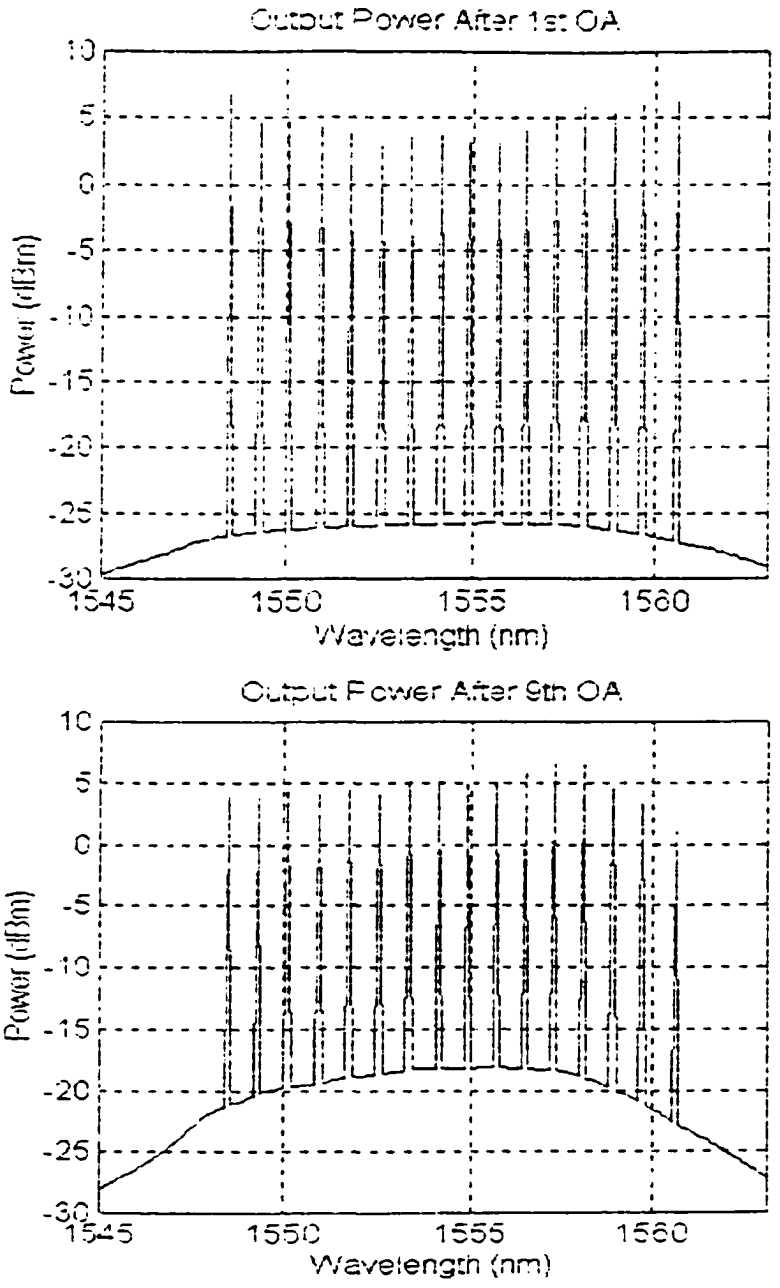

Figure 4.2. Experimental results of 16 x 2.5 Gbit's over 800 Km transmission system

4.3 Simulation Results

Due to the limited sources, we can not demonstrate a higher capacity system. But, with the use of the simulation tool, we can extend our system development to larger number of wavelengths and different amplifier configurations. By using the same SMF parameters, the Erbium fiber characteristics, power per channel values, and outside plant loss, we have been able to successfully match the simulation results to the measurements within a certain degree of accuracy.

As shown in figure 4.3, the measurement and simulation results for SNRs are within a 1 dB differential after the 9th amplifier, and the shape of the spectrum is almost the same. The power per channel varies from 0.5 dB to 1.5 dB, where the highest divergence is experience in the shorter wavelengths. The differences between simulation and measurement can be attributed to the following factors:

- Pump wavelength dependency.
- Erbium fiber absorption and emission coefficients.

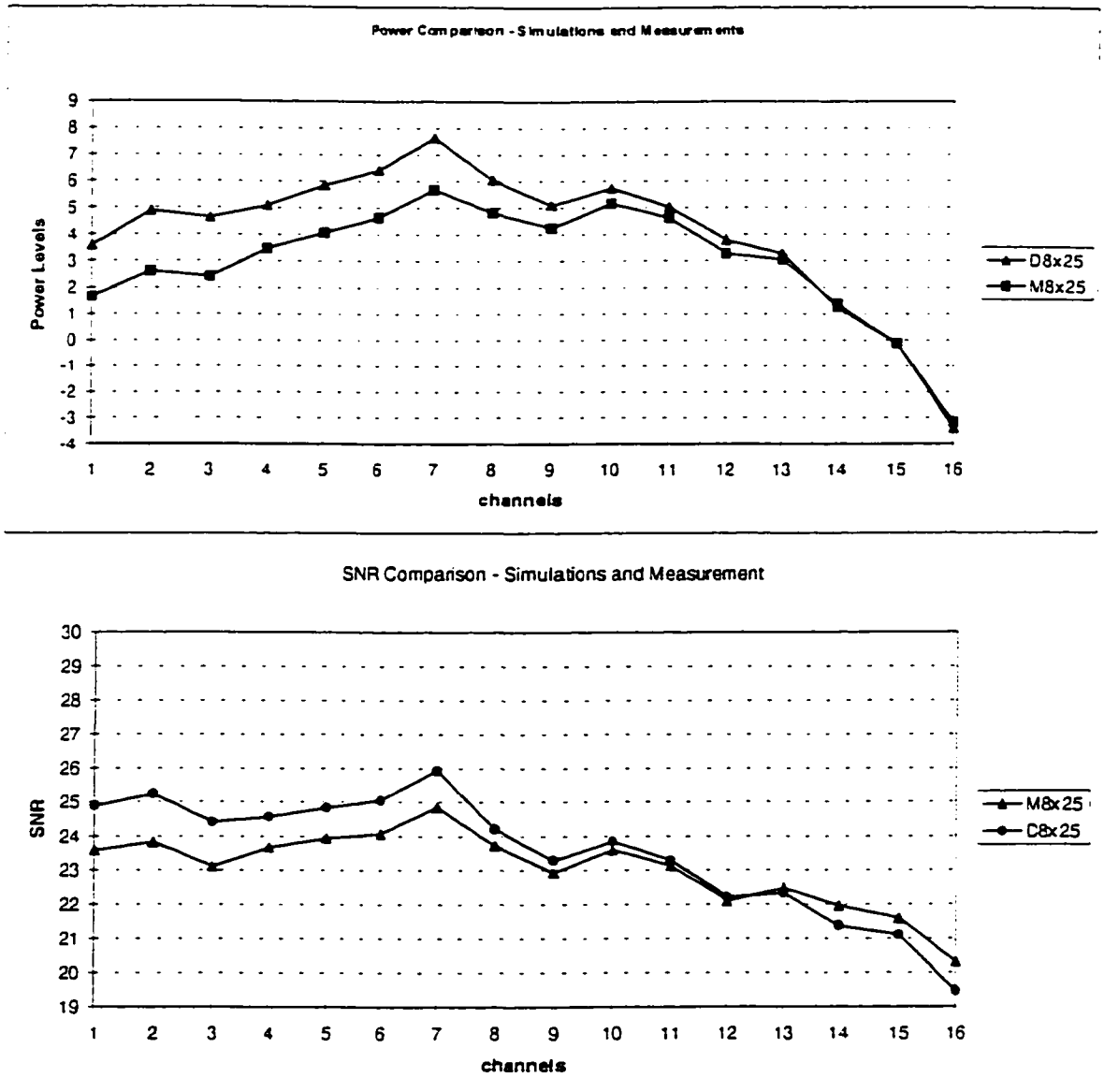

Figure 4.3. Simulation vs. Measurement results. M8x25: Measurement after 9th OA with 25 dB span loss. D8x25: Simulation after 9th OA with 25 dB span loss.

CHAPTER 5

Feasibility of Tb/s DWDM Transmission Systems

5.1 Introduction

The design of ultra-high capacity DWDM transmission systems and optical networks is currently constrained by the limited bandwidth available from erbium-doped fiber amplifiers (EDFAs). The usable bandwidth is limited to about 12-nm because of the highly structured gain spectrum. With gain equalization filters (GEFs) [1], this gain bandwidth can be extended to between 35 and 40 nm (about 1525 to about 1565 nm) [2-3]. Since the gain drops sharply below 1525 nm or above 1565 nm, it is not practical to further increase the gain bandwidth with GEFs. As we scale up the number of wavelengths in WDM systems, the spacing between wavelengths will decrease and the crosstalk among channels will increase. This system

crosstalk will eventually limit the scaling capacity of DWDM networks required, for instance, for the efficient implementation of the Next-Generation Internet (NGI) backbone transport facilities.

To further increase capacity with a channel spacing compatible with practical filtering technology, as well as to increase wavelength routing network capability, the number of channels must grow. It would also be advantageous to be able to access one or more of the optical channels at any amplifier site in a WADM configuration. The WADM configuration must include both fixed and reconfigurable optical add/drop multiplexers. This will require developing novel ultra broad-band silica-based EDFA configurations with flexible and scalable optical add/drop capabilities along with a compatible filtering technology capable of providing 60-80 nm of optical bandwidth while keeping both the spectral gain variations and the inter-channel cross-talk as small as possible.

The purpose of this chapter is three fold:

1. We will investigate and develop several novel two-band EDFA configurations capable of providing as large as 80-nm of optical bandwidth using only silica-based EDFAs. This is achieved by combining the gain in the conventional wavelength range between 1525 and 1565 nm (called S-band in this work) and that in the long wavelength range between 1570 and 1600 nm (called L-band here). Each configuration consists of two parallel dual-stage

silica-based EDFA, where each dual-stage is independently optimized. Such configurations offer a practical route to removing the bandwidth limits which currently constrain the design of flexible WDM systems and networks. With 80 nm of bandwidth, this EDFA configuration will be able to accommodate 100 WDM channels with the proposed ITU standard channel spacing of 100 GHz.

These configurations must be capable of satisfying the following:

- Low-noise and high output power.
- Gain flatness should be independent of the operating conditions (signal and pump power levels, etc.).
- Maintain constant per-channel output power with a minimally degraded SNR, regardless of the number of channels present, over a wide dynamic range of input signal levels.
- Amplify and add/drop any number of wavelengths ranging from 1-100.
- Flexible for graceful in-service upgrade to a maximum of 100 WDM channels along with the smooth evolution in increasing the bit rate per channel from OC-12 to OC-192.

We will examine the various technological difficulties facing EDFA cascades with multi-wavelength handling capabilities. Two related fundamental problems will be addressed:

(i) spectral gain non-uniformity or "gain equalization". This is one of the major remaining problems facing multiwavelength transmission systems with fiber-amplifier cascades. When wavelength-multiplexed signals traverse a single amplifier, the individual channels experience various gains determined by the spectroscopy of the gain medium, the fiber length, and the signal and pump power levels. In a single amplifier, these spectral gain variations are generally modest, but they accumulate from stage to stage in a cascade, rapidly growing too large to allow adequate noise performance at the less-favored signal wavelengths.

(ii) noise accumulation in high data rate WDM repeater chains.

The main objective is to ensure sufficient gain flatness to permit amplifiers to be cascaded while maintaining acceptable inter channel power variations and signal-to-noise ratios at all wavelengths.

2. Using an optimum two-band EDFA configuration along with a dispersion compensating fiber (DCF), we will show the viability of 64-100 DWDM 10 Gb/s channels transmission with 100 GHz spacing over 1000 km of standard SMF.

3. The feasibility of using two new features, crucial for broadband long-haul DWDM transmission systems, to equalize (flatten) the passband of cascaded EDFAs, will be examined. First, long-period fiber gratings will be used to flatten the gain and broaden the optical

bandwidth of a two-stage mid-amplifier pumped EDFAs. Second, mid-amplifier attenuators will be used to permit the EDFAs to be operated with broadband, flat gain over a wide dynamic range of input powers which is necessary to accommodate variations encountered in system span losses. Using these two new features, we will show the viability of sixty four 2.5 Gb/s DWDM channels transmission with 50 GHz spacing over 1056 km of standard SMF.

5.2 *Two-Band Silica-Based EDFAs Architectures*

Fig. 5.1 shows one architecture of the proposed two-band EDFA configuration. It consists of two parallel dual-stage silica-based EDFA, where each dual-stage is independently optimized first for output power and secondly for gain flatness over the 40-nm signals bandwidth. Circulators and broad band fiber Bragg gratings that reflect the S-band are used to demultiplex and multiplex the two bands before and after amplification, respectively. Thus, the two bands are amplified separately and are recombined afterwards. The circulators also act as isolator. Both bands use the same type of silica-based fibers but with longer amplifier lengths for the L-band.

A WADM is assumed to be located between the dual-stage EDFA of each band, as shown in Fig. 5.1. Each WADM, as shown in Figs. 5.2 and 5.3, consists of short-period fiber grating filters along with circulators and a given number of wavelength selective elements depending on the number of wavelengths to be added/dropped at a given node, to perform the WADM capabilities. For a fixed WADM configuration, the number of short-period grating filters will depend on the wavelength drop/add assignment plan. However, for a fully reconfigurable WADM, the number of short-period grating filters should equal the total number of wavelengths passing through the EDFA configuration. Another critical criterion that must be met in the design of our proposed EDFA configuration is its flexibility for graceful in-service upgrade to a maximum of 100 WDM channels along with the smooth evolution in increasing the bit rate per channel from OC-12 to OC-192.

Fig. 5.4 shows a second architecture of the proposed split-band EDFA configuration. This architecture is exactly the same as that of Fig. 5.1, except that the propagation direction of the L-band is now in the counter direction of that of the S-band and therefore the broad band fiber Bragg gratings that are used to demultiplex and multiplex the two bands are no longer needed. This means that this configuration can be used in a bi-directional system with just a single fiber. If this configuration were to replace that of Fig. 5.1 at each node of a DWDM transmission system, the transmission system will become a bi-directional 2-fiber ring. We will compare the end-to-end performance of a DWDM transmission system comprising the first EDFA

configuration of Fig. 5.1 at each of its node with that comprising this configuration at each of its node. This comparison should be based on both the technological and economical aspects.

Note that the transition range of the broadband fiber Bragg gratings between reflection and transmission is about 0.5-nm [4], as shown in Fig. 5.5. It is unlikely that significant improvement can be made on reducing the current 0.5 nm guardband. In order to make coherent crosstalk negligible, an isolation of 30 dB or more is needed, which requires 15 dB rejection for the double pass configuration in Fig. 5.1. The rejection ratio of more than 25 dB of current broad band Bragg gratings should be sufficient to be used in optical communication networks. Note also that the architecture of Fig. 5.4 does not require broad band fiber Bragg gratings.

Several other candidate architectures will also be examined and their performances will be compared with those of the above two architectures. For instance, one architecture can use two sections, one common section where all channels can pass through one amplification stage, and the second section can be the split section where channels are split into two bands.

5.2.1 Modeling the Two-Band EDFA Configuration

We will simulate the overall performance of several different split-band EDFA architectures with different pumping schemes, pumping wavelength, pumping power, input signal levels, and WADM capabilities for each band. It might be just 980-nm pumping, 1480-nm

pumping, and/or a combination of both 980-nm and 1480-nm pumping wavelength, forward pumping scheme, backward pumping scheme, and/or a bi-directional pumping schemes. For a given architecture, each dual-stage will be independently optimized first for output power and secondly for gain flatness over the 40-nm signals bandwidth. Different wavelength assignments for each band will also be examined, i.e. 1520-1560-nm/1525-1565 nm for the S-band and 1565-1605-nm/1570-1610-nm for the L-band, in order to determine the optimum wavelength assignments for each band.

5.3 64/100 x 10 Gbit/s DWDM Transmission System with 50 and/or 100 Ghz Channel Spacing

5.3.1 Introduction

This work simulates a system with 64 WDM 10 Gb/s channels over 1000 km of standard single mode fiber (SMF) with 100 km repeater spans. Dispersion compensation was handled using dispersion compensating fiber (DCF) between the two stages of each amplifier. This was done since most of the fiber in use is standard SMF. In addition, the high dispersion of this fiber virtually eliminates nonlinear interactions between channels, and therefore, the effects of nonlinearities on the system performance are reduced and were not taken into account in this work. A perfect dispersion compensation is assumed. That is, the effect of

chromatic dispersion on the system performance is ignored; only the loss of the dispersion compensator is taken into account. The amplifiers in this system are two-stage, dual-band, silica-based EDFAs, allowing separate compensation for each band. Also, each band can be used independently, allowing for modular growth. No attenuators were used.

5.3.2 The System Model

The system model consists of 64 WDM channels subdivided equally into two subbands, the C-band and the L-band. 32-channels are spaced 100-GHz apart in the 1532.4 (channel 1) to 1557.2-nm (channel 32) amplifier C-band and the remaining 32-channels are also spaced 100-GHz apart in the 1574 (channel 33) to 1598.8-nm (channel 64) amplifier L-band. Circulators and broad band fiber Bragg gratings that reflect the C-band are used to demultiplex and multiplex the two bands before and after amplification, respectively. Thus, the two bands are amplified separately and are recombined afterwards. Both bands use the same type of silica-based fibers but with longer amplifier lengths for the L-band.

The two-band EDFA configuration, shown in Fig. 5.6, consists of two parallel dual-stage silica-based EDFA, where each dual-stage is independently optimized first for output power and secondly for gain flatness over the 24.8-nm signals bandwidth [5]. The C-band dual-stage EDFA used in the simulation is co-pumped with 250 mW of pump power at 980-nm in stage 1 and with 410 mW at 980-nm in stage 2. The L-band dual-stage EDFA is bi-directionally

pumped with 200 mW of pump power in the forward direction, 100 mW in the backward direction at 980-nm in stage 1 and with 270 mW of pump power in the forward direction, 200 mW in the backward direction at 980-nm in stage 2. The design of both amplifier stages for each band was chosen to produce an average dual-stage net gain of about 25 dB. EDF stages of the L-band are six times longer than that of the C-band. Consequently, an additional 110 mW of pump power was required in order to produce an average L-band dual-stage net gain equal to that of the S-band (25 dB).

The alumino-germano silicate EDF used in the simulation is a commercially available fiber designed for high output power. A long-period fiber grating filter gain equalizer is located between the stages of both the C and L arms along with an isolator and a DCF. The computed ideal filter transmission characteristics for each band was determined based on the optimization method reported in [6]. The C-band filter used produces about 10-13 dB attenuation near 1530-nm while that of the L-band produces only about 1-1.5 dB attenuation near 1580-nm. Using the optimization method reported in [6], the intrinsic C-band/L-band dual-stage EDFA spectral gain variation of 5.6 dB/3.3 dB over the 24.8 nm bandwidth were reduced to less than 0.01 dB for both bands. The total inter-stage losses for each band is the sum of 3 dB component losses and 8 dB DCF loss = 11 dB. The input signal levels assumed in the calculations are -17.5 dBm/channel at the input of the first stage of each band. The total input and output coupling loss for each band is assumed to be 3 dB. The NF is calculated to be

below 5.6 dB and 5.5 dB at an average dual-stage net gain of about 25 dB for all wavelengths across the WDM signals bandwidth for the L-band and the C-band, respectively.

5.3.3 Results and Discussion

The transmission fiber consisted of ten 100 km spans of standard SMF having an average chromatic dispersion of +17 ps/km-nm and an average attenuation of 0.25 dB/km, for a total transmission distance of 1000 km. Each span is followed by 16 km of DCF, located between the dual-stage EDFA of each band, having an average chromatic dispersion of -105 ps/km-nm and an average attenuation of 0.5 dB/km. The optimum span loss between amplifiers is set equal to the average dual-stage amplifier gain of 25 dB [5]. This corresponds to 100 km of fiber at 0.25 dB/km.

The signal and ASE power accumulation along the EDFA chain is determined based on the spectrally resolved numerical model of Ref. [7]. The accumulated optical signal-to-noise ratio (SNR) reported here is the ratio between the signal level and the accumulated ASE noise power in a 0.2-nm optical bandwidth. The end-to-end system performance is estimated from the optical (SNR), which must be more than 18 dB (0.2-nm resolution) to achieve a bit-error ratio of 10^{-14} at 10 Gb/s [8]. Fig. 5.7 shows calculations of the output signal levels and the accumulated ASE power in a 0.2-nm optical bandwidth immediately after the 1st and 11th amplifier along the cascade. The SNR is greater than 32 dB after the first amplifier, and

remains greater than 22 dB for all channels after the 11^{th} amplifier (total transmission distance of 100 x 10 = 1000 km). Both the output signal levels and SNRs are nearly equal after the 11^{th} amplifier, with less than 0.3 dB inter-channel power spread and a 1dB SNR differential among all 64 channels. After 21 amplifiers, the total system gain is 525 dB, the SNR remains greater than 19 dB for all channels after the 21^{th} amplifier (total transmission distance of 100 x 20 = 2000 km), the SNR differentials are only 2 dB, and the gain variations are only about 1 dB, suitable for 10 Gb/s operation/ channel. No mid-amplifier attenuators nor transmitter pre-emphasis were used to achieve these results.

It should be emphasized that the entire simulation presented here is based on the assumption that a real long-period fiber grating filter could be constructed that exactly matches the computed filter shape used in the simulation. The validity of this assumption has been demonstrated using long-period grating filters in system experiments [1-3], where a long-period grating filter was fabricated to exactly match the computed ideal filter shape designed to produce a gain-flattened silica-based EDFA over a 40-nm bandwidth [3]. To test how accurately a fabricated filter must fit the ideal shape used in the simulation, all the above calculations were repeated using filters with transmission characteristics that deviate $\pm$ 0.5-2 dB from that of the corresponding ideal filter over the wavelength range of interest. For the worst case of 2 dB deviation, the SNR remains greater than 19 dB for all channels after the 11^{th} amplifier, indi-

cating that a fabrication accuracy within 0.5-2 dB is still suitable for 10 Gb/s operation/channel. However, the inter-channel power spread is now up to 3 dB and 12 dB, at o.5 dB and 2 dB deviations. respectively.

To test the effect of the span loss variations on the simulation results obtained using the optimum span loss (25 dB), all the above calculations were repeated again using the computed ideal filter shape for each band, but with a span loss that deviate $\pm$ 1-3 dB from that of the optimum. The SNR at $\pm$ 2 dB span loss variations remains greater than 18.7 dB for all channels after the 11^{th} amplifier, indicating that 10 Gb/s transmission can tolerate such span loss variations. However, at $\pm$ 3 dB span loss variations both the SNR and the inter-channel power spread are no longer acceptable for 10 Gb/s operation.

In conclusion, using computer simulation, we have shown the viability of 64 WDM 10 Gb/s channels transmission over 1000 km of standard SMF using novel silica-based two-band EDFA configuration and dispersion compensating fiber (DCF).

5.4 64x2.5 Gb/s DWDM Transmission System With 50 Ghz Channel Spacing

5.4.1 Introduction

Dense wavelength division multiplexed (DWDM) transmission systems are now being deployed on a very large scale in commercial networks. The transmission of these long-haul DWDM systems can be limited by the finite bandwidth of the silica-based Erbium-Doped Fiber Amplifier (EDFA) repeaters and the nonlinear interactions between channels. To further increase capacity with a channel spacing compatible with practical filtering technology, as well as to increase wavelength routing network capability, the number of channels must grow and this will require a new design of ultraflat EDFA configurations. Capacity of thirty two 10 Gb s channels transmitted 640 km [9] and thirty two 5 Gb/s channels transmitted 9300 km [10] have been demonstrated in system experiments using silica-based EDFA repeaters. Experimental long-haul transmission has also been reported using erbium-doped fluoride fiber amplifiers (EDFFAs), which offer an optical bandwidth of about 24-nm [11].

In this work, using two different long-haul DWDM transmission system configurations, we simulate transmission of sixty four 2.5 Gb/s WDM channels with 50 GHz spacing over 1056 km of standard single mode fiber (SMF). Each configuration uses gain-flattened silica-based dual-stage EDFA, long-period fiber grating filters, and dispersion compensating fibers (DCFs). The DCFs are assumed to be located before and after the first amplifier stage for the first (config. I) and second (config. II) configurations, respectively. The task of compensating for chromatic dispersion has been addressed here by using DCFs, because of their simplicity

of the exact dispersion adjustment, so that a perfect dispersion compensation is assumed. That is, the effect of chromatic dispersion on the system performance is ignored; only the loss of the dispersion compensator is taken into account. Standard SMF was chosen as most of the existing optical networks are based on this type of fiber. In addition, standard SMF is virtually unaffected by nonlinear interactions between channels due to its high dispersion. Therefore, nonlinear effects were not taken into account in this work.

5.4.2 The System Model

The system model for the two system configurations simulated here, shown in Fig. 5.8, consists of sixty four WDM channels spaced 0.4-nm apart in the 1535.2 (channel 1) to 1560.4-nm (channel 64) amplifier band. The ultraflat EDFA configuration used in the simulation consists of a dual-stage EDFA, counter-pumped with 90 mW of pump power at 980-nm in stage 1 and copumped with 90 mW at 980-nm in stage 2. The alumino-germano silicate EDF used in the simulation is a commercially available fiber (Lucent fiber). A long-period grating filter is located between the stages along with an isolator. The ideal filter spectrum is computed based on the following optimization method [12]:

For a given total input power, $P_{in}^{(2)}$, at the input of the 2nd stage, determine the intrinsic 64 WDM signal gain spectrum, $G_{intrinsic}(\lambda)$, assuming an equal input signal level/ channel and forward pumping scheme with 90 mW of pump power at 980-nm pumping.

Determine the input signal level channel, $P^{(2)}_{in\_flat}(\lambda)$, required to produce a flat output spectrum over the 25.2-nm signals bandwidth at the output of the 2nd stage by first using the normalized 64 WDM signal gain spectrum. $G_{normalized}(\lambda)$, defined as:

$$G_{normalized}(\lambda) = G_L\, G_{intrinsic}(\lambda); \qquad \text{then,}$$

$$P^{(2)}_{in\_flat}(\lambda) = G_{normalized}(\lambda) * P^{(2)}_{in} \cdot \sum_{\lambda} G_{normalized}(\lambda)$$

where G_L is the least-favored signal gain from among all of the 64-signal wavelengths and

$$P^{(2)}_{in} = \sum_{\lambda=1}^{\lambda=64} P^{(2)}_{in\_flat}(\lambda)$$

Determine the 64 WDM output power spectrum, $P^{(1)}_{out}(\lambda)$, of the 1st stage assuming an input signal level of - 25 dBm channel and backward pumping scheme with 90 mW of pump power at 980-nm pumping.

Determine the transmission characteristics of the long-period fiber grating filter, $T(\lambda)$, by using the following equation:

$$P^{(1)}_{out}(\lambda) * (\text{total interstage losses}) * T(\lambda) = P^{(2)}_{in\_flat}(\lambda) \qquad (1)$$

The total interstage losses of configuration II is the sum of 3 dB component losses and 6.2 dB DCF loss = 9.2 dB. On the other hand, the total interstage losses of configuration I is only equal to the component losses = 3 dB. Note the constraint imposed on $P^{(1)}_{out}(\lambda)$ in Eq. (1), that is, in order to determine the appropriate values of $T(\lambda)$, $P^{(1)}_{out}(\lambda)$ must satisfy the following relationship: $P^{(1)}_{out}(\lambda)$ * (total interstage losses) $\geq P^{(2)}_{in,flat}(\lambda)$

The design of both amplifier stages, in each configuration, was chosen to produce an average dual-stage net gain of about 24 dB at the expense of noise figure (NF) penalty. Consequently, the EDF stages of configuration II were longer than that of configuration I in order to take into account the additional inter-stage loss introduced by the DCF. The internal NF is calculated to be below 4.8 dB and 5.9 dB for all wavelengths across the WDM signals bandwidth for configurations I and II, respectively. The computed ideal filter transmission of config. I is plotted in Fig.5.9. As can be seen from the Fig., the filter used produces about 10-12 dB attenuation near 1530-nm. The transmission characteristics of the filter used in configuration II has almost the same spectrum shape as that of configuration I, but the filter produces about 1-2 dB higher attenuation over the entire spectrum. Using the above optimization method, the dual-

stage EDFA spectral gain variation of 5.5 dB over the 25.2 nm bandwidth was reduced to less than 0.15 dB, for both configurations. As long as the gain and total fiber length remained the same, the long-period grating filter properly flattened the EDFA spectrum.

It should be emphasized that the entire simulation presented here is based on the assumption that a real long-period fiber grating filter could be constructed that exactly matches the computed filter shape used in the simulation. The validity of this assumption has been demonstrated using long-period grating filters in system experiments [1-2, 3], where a long-period grating filter was fabricated to exactly match the computed ideal filter shape designed to produce a gain-flattened silica-based EDFA over a 40-nm bandwidth [3]. As will be shown below, a filter with transmission characteristics that is within $\pm$ 0.5 dB from that of the ideal filter over the wavelength range of interest (1520-1570 nm), produces almost the same final cascade performance results as that achieved using the ideal filter.

5.4.3 Results and Discussion

The signal and ASE power accumulation along the EDFA chain is determined based on the spectrally resolved numerical model of Ref. [7]. The accumulated optical signal-to-noise ratio (SNR) reported here is the ratio between the signal level and the accumulated ASE noise power in a 0.2-nm optical bandwidth. The end-to-end system performance is estimated from

the optical (SNR), which must be more than 14.5 dB (0.2-nm resolution) to achieve a bit-error ratio (BER) of 10^{-14} at 2.5 Gb/s [8].

To carry out a proper comparison between the transmission performance of the two configurations, the number of cascaded dual-stage amplifiers in the two cases is adjusted so that the minimum SNR is near 14.5 dB in each case. This in turn will determine the maximum adequate transmission distance that can be achieved in each case. The transmission fiber of both configurations consisted of spans of standard SMF having an average chromatic dispersion of + 17 ps/km-nm and an average attenuation of 0.25 dB/km. Each span is followed by 12 km of DCF having an average chromatic dispersion of -95 ps/km-nm and an average attenuation of 0.515 dB/km.

For config. II, the span loss between amplifiers is set equal to the average dual-stage amplifier gain of 24 dB. This corresponds to 96 km of fiber at 0.25 dB/km. Fig. 5.10 shows calculations of the output signal levels and the accumulated ASE power in a 0.2-nm optical bandwidth immediately after the first and 12^{th} amplifier along the cascade. The SNR is greater than 26 dB after the first amplifier, and remains greater than 14.6 dB for all channels after the 12^{th} amplifier (total transmission distance of 96 x 11 = 1056 km). Both the output signal levels and SNRs are nearly equal after the 12^{th} amplifier, with less than 1.2 dB inter-channel power spread and a 0.2 dB SNR differential.

For config. I, the span loss between amplifiers is set equal to the average dual-stage amplifier gain of 24 dB. This corresponds to 70 km of fiber at 0.25 dB/km plus the DCF loss of about 12 km x 0.515 dB/km = 6.2 dB, and in this case, 16 cascaded amplifiers are needed to achieve a total transmission distance of 1050 km. After the cascade, the SNR remains greater than 14.5 dB for all channels. Both the output signal levels and SNRs are nearly equal after the 16^{th} amplifier (total transmission distance of 15 x 70 = 1050 km), with less than 1.7 dB inter-channel power spread and a 1.5 dB SNR differential. This indicates that the overall transmission performance is almost the same as that of config. II, although config. I uses 4 more amplifiers than config. II to achieve that performance.

To test how accurately a fabricated filter can be made to fit the desired ideal shape used in the simulation, all the above calculations were repeated again, however, using a filter with transmission characteristics that deviate $\pm$ 0.5 dB from that of the ideal filter over the wavelength range of interest (1520-1570 nm). The results obtained are almost the same as those obtained above using the computed ideal filter shape, indicating that a fabrication accuracy within 0.5 dB is satisfactory.

In conclusion, we have simulated transmission of 64 x 2.5 Gb/s WDM channels spanning 25.2 nm over 1056 km of standard SMF for two different configurations using entirely silica-based ultraflat EDFAs. The transmission performance of both configurations could be

improved by the use of mid-amplifier attenuators that would permit the EDFA to operate over a wide dynamic range of input signal levels which is necessary to accommodate variations encountered in system span losses.

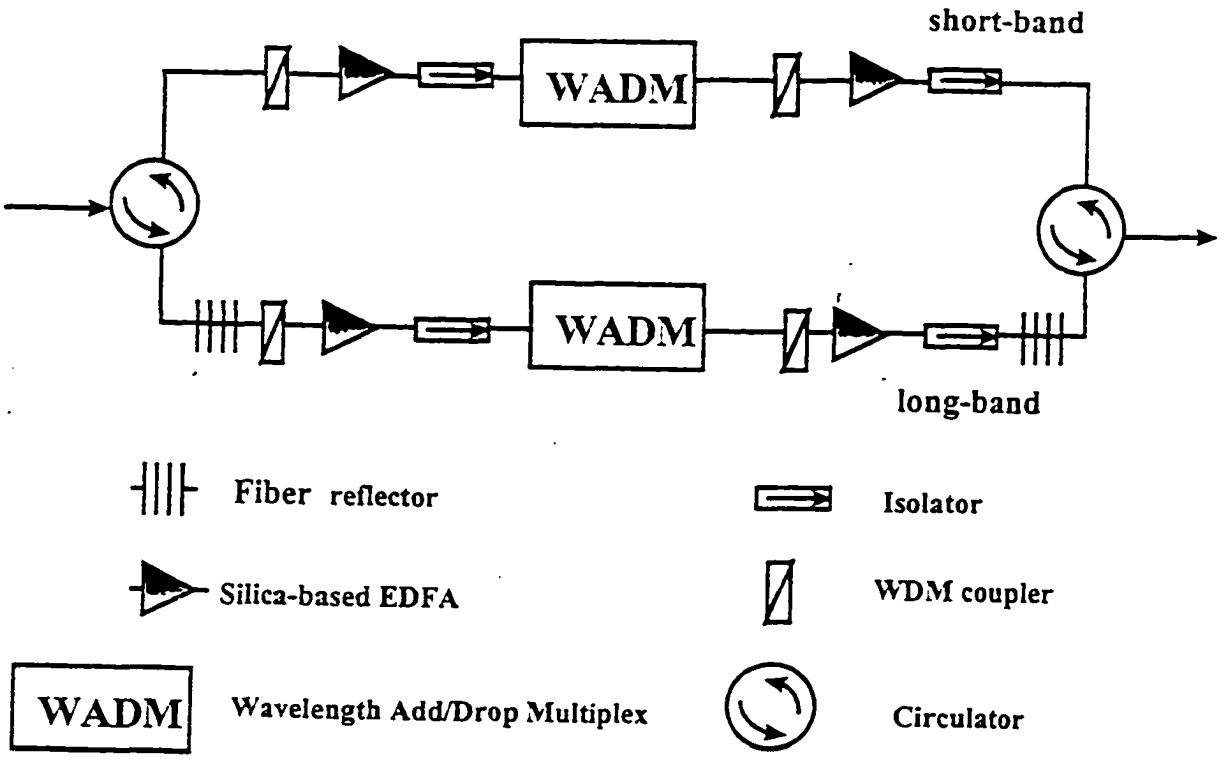

Figure 5.1. Schematic diagram of one architecture of proposed dual-band EDFA.

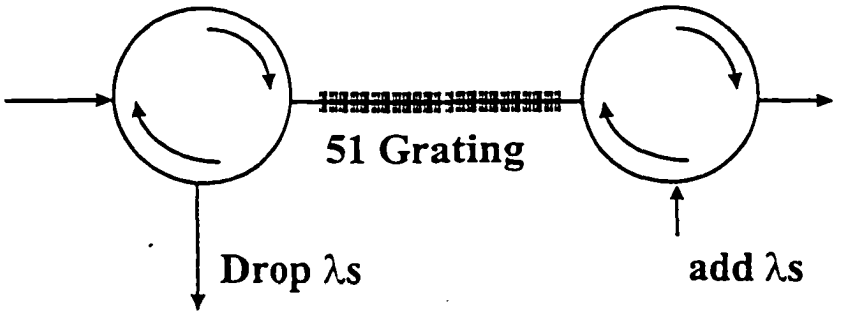

•Require ultra-wideband EDFA configuration, i.e. 50 λ's with 100GHz channel spacing

Figure 5.2. Add/Drop design for 51 λ.

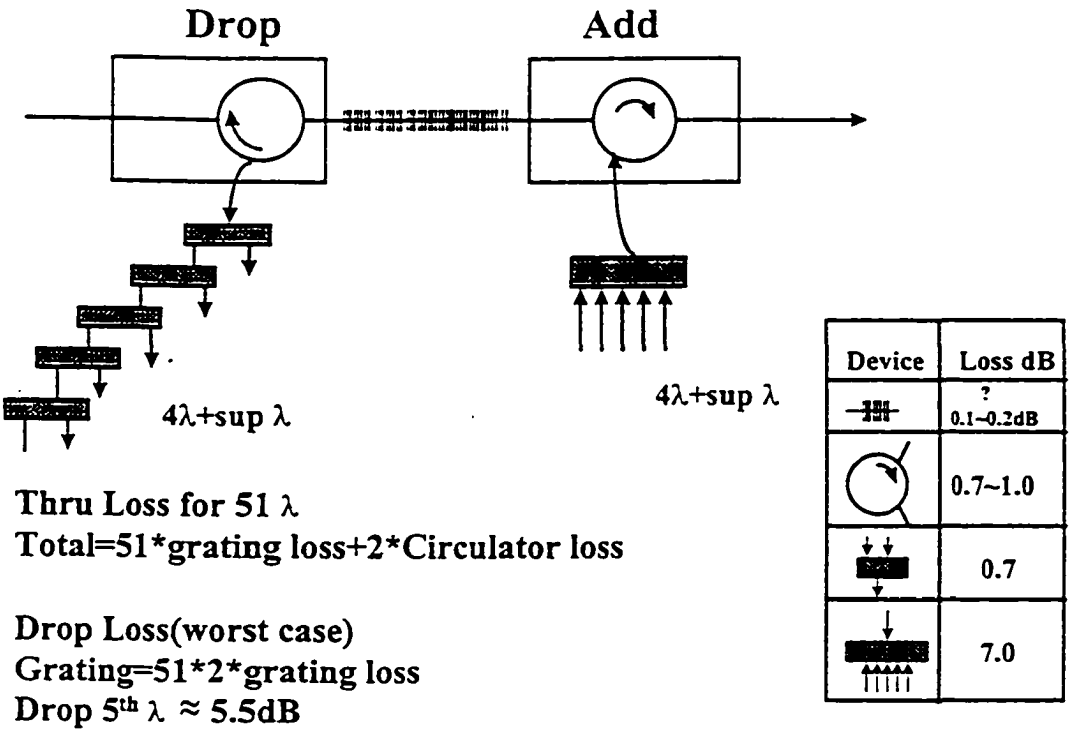

Figure 5.3. 51 λ Add/Drop

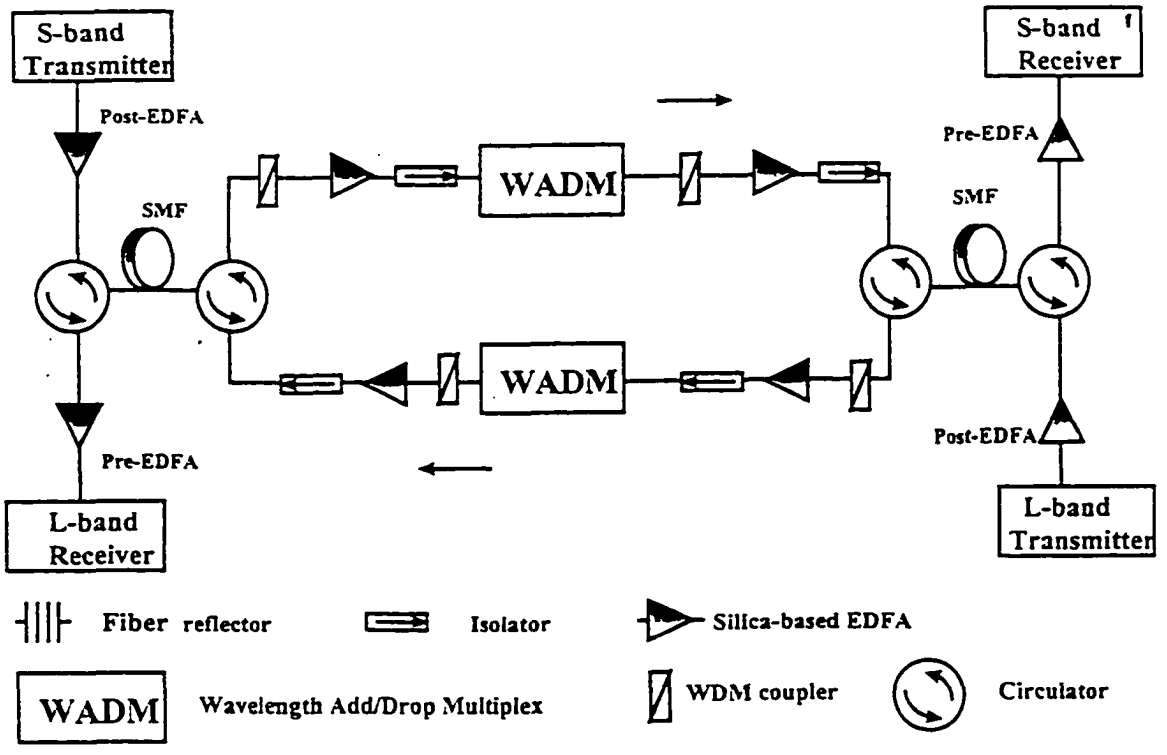

Figure 5.4. Bidirectional schematic diagram of a second architecture of proposed dual-band EDFA configuration using only one fiber.

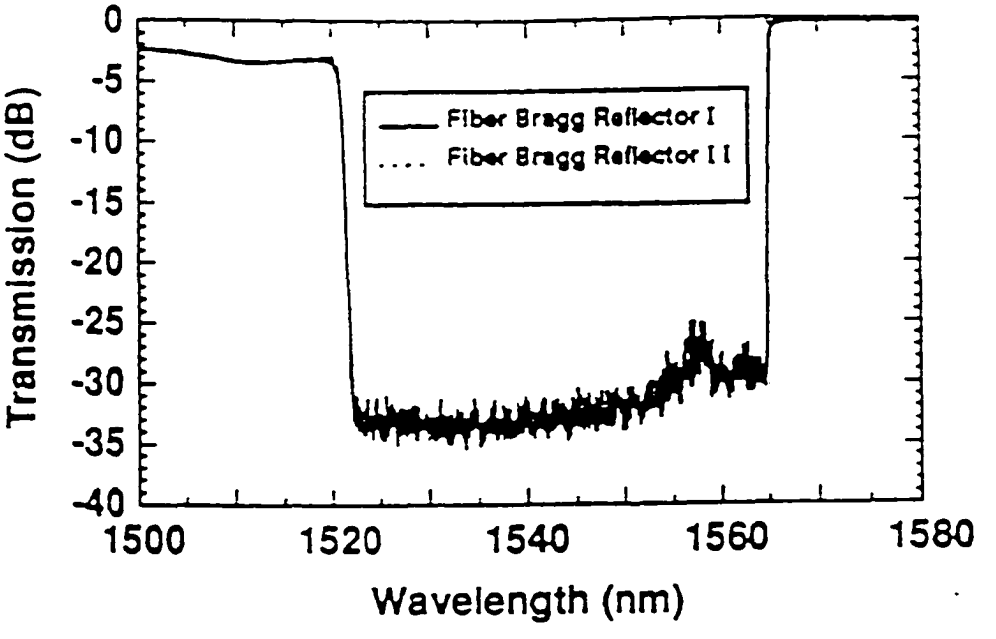

Figure 5.5. Two overlapped transmission spectra of broadband bragg fiber gratings used in ultra-broadband EDFA configurations. The transition region between reflection of the S-band and the transmission of the L-band is about 0.5 nm.

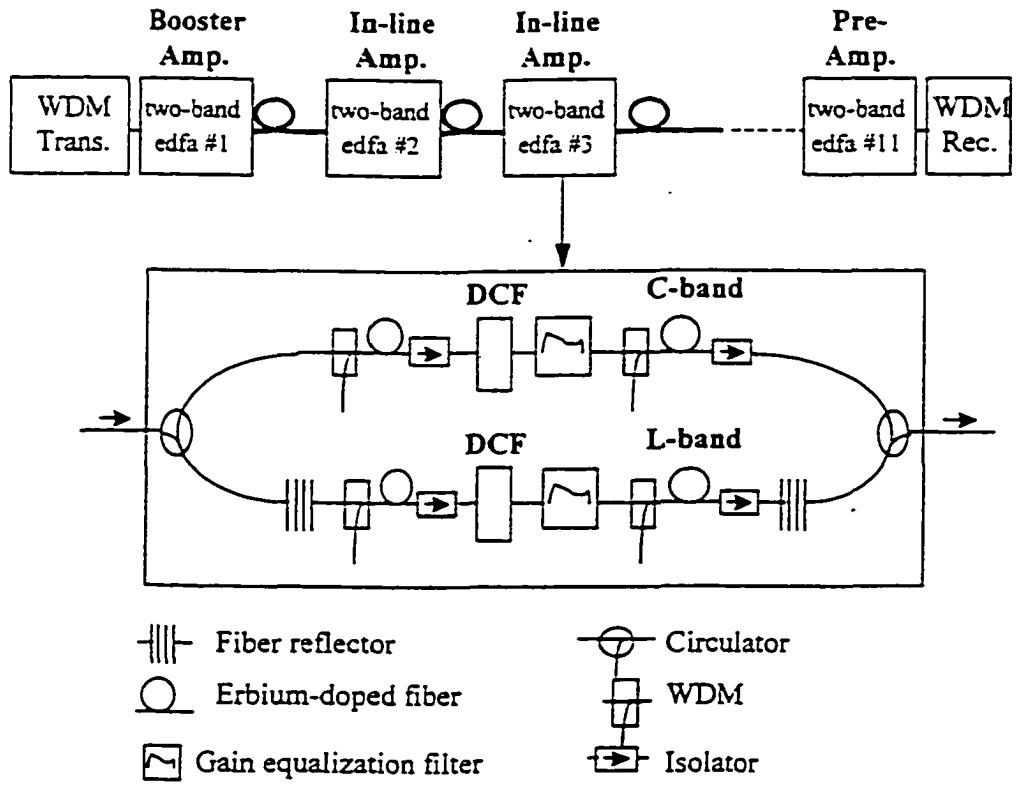

Figure 5.6. Two-band EDFA configuration.

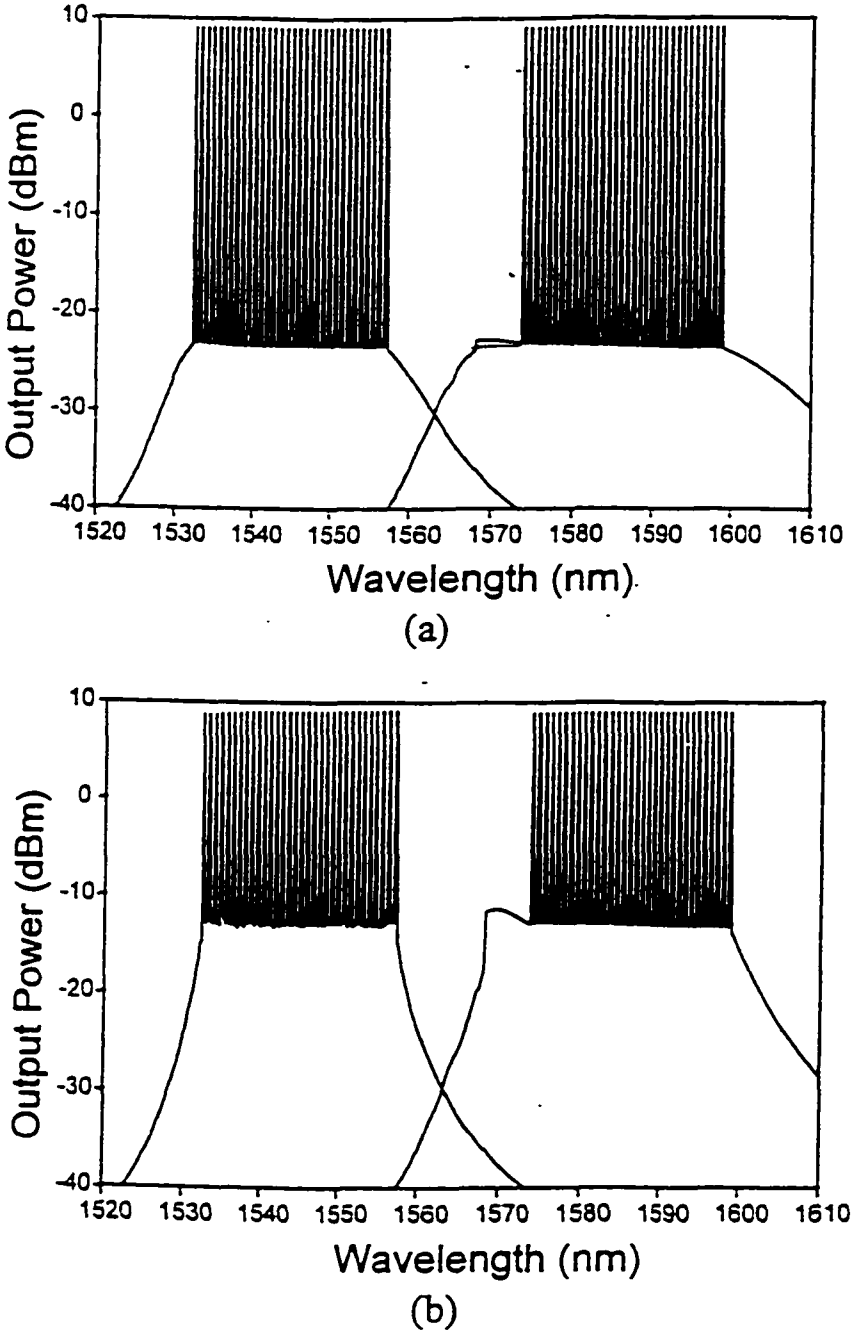

Figure 5.7. (a) Output power after the 1st EDFA. (b) Output power after the 11th EDFA.

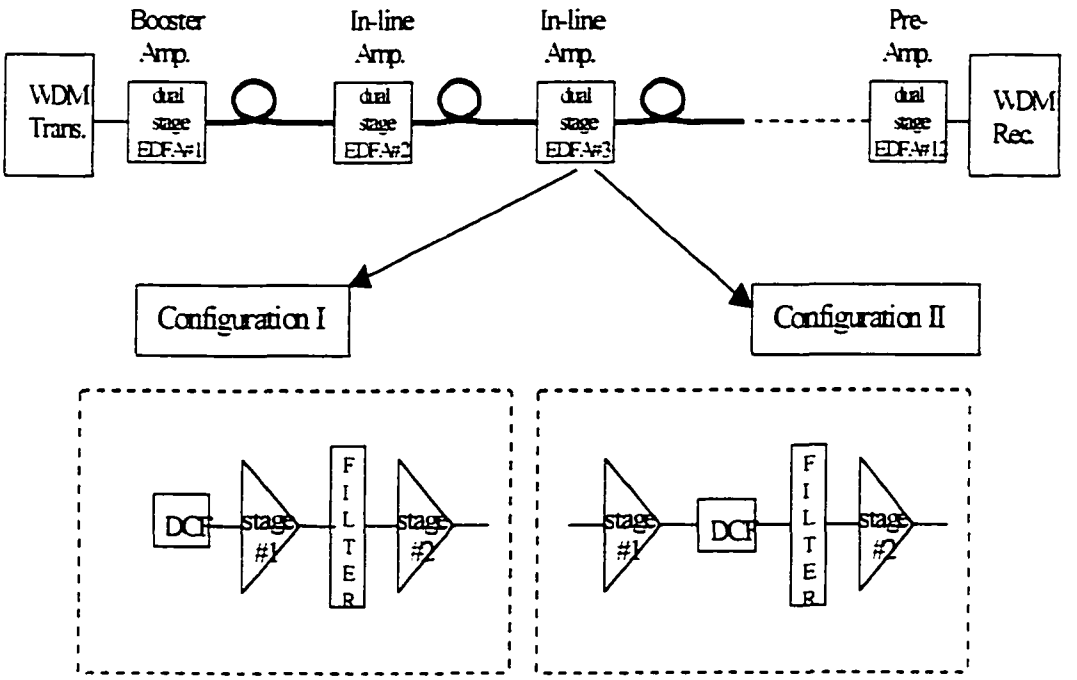

Figure 5.8. Two system configurations for the transmission of 64 channels at 50 Ghz channel spacing.

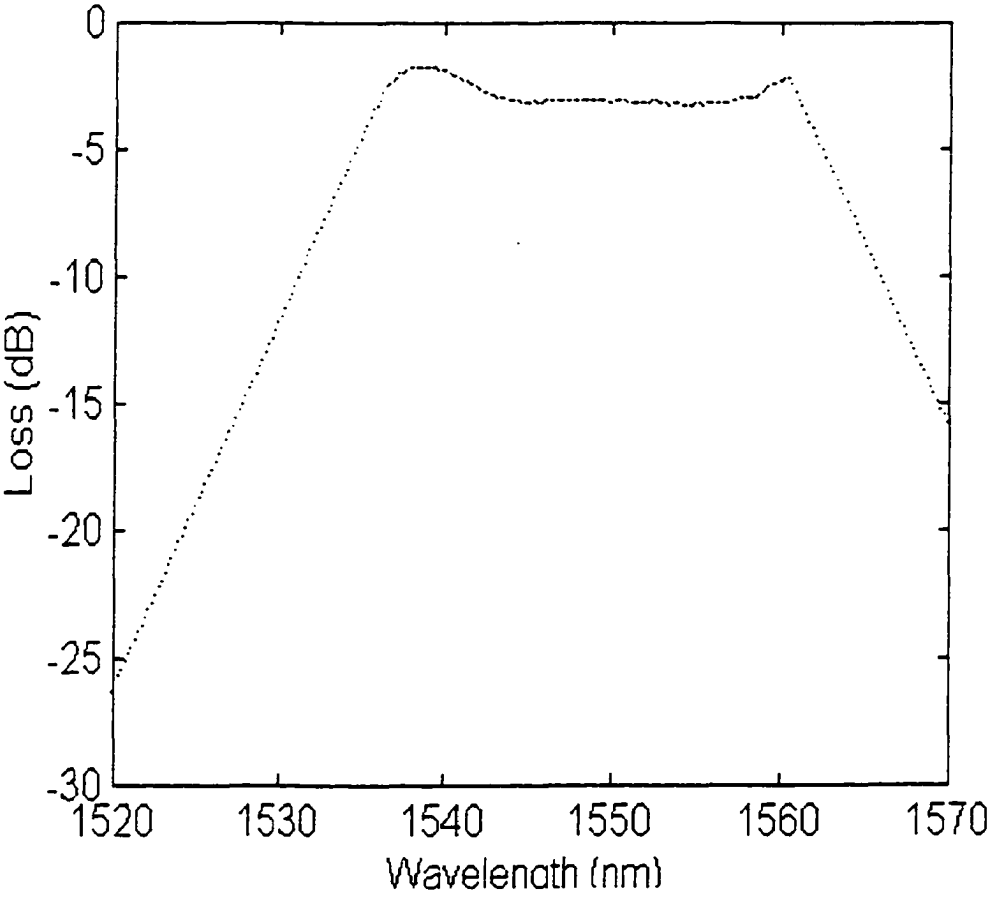

Figure 5.9. Transmission characteristics of a long-period fiber grating.

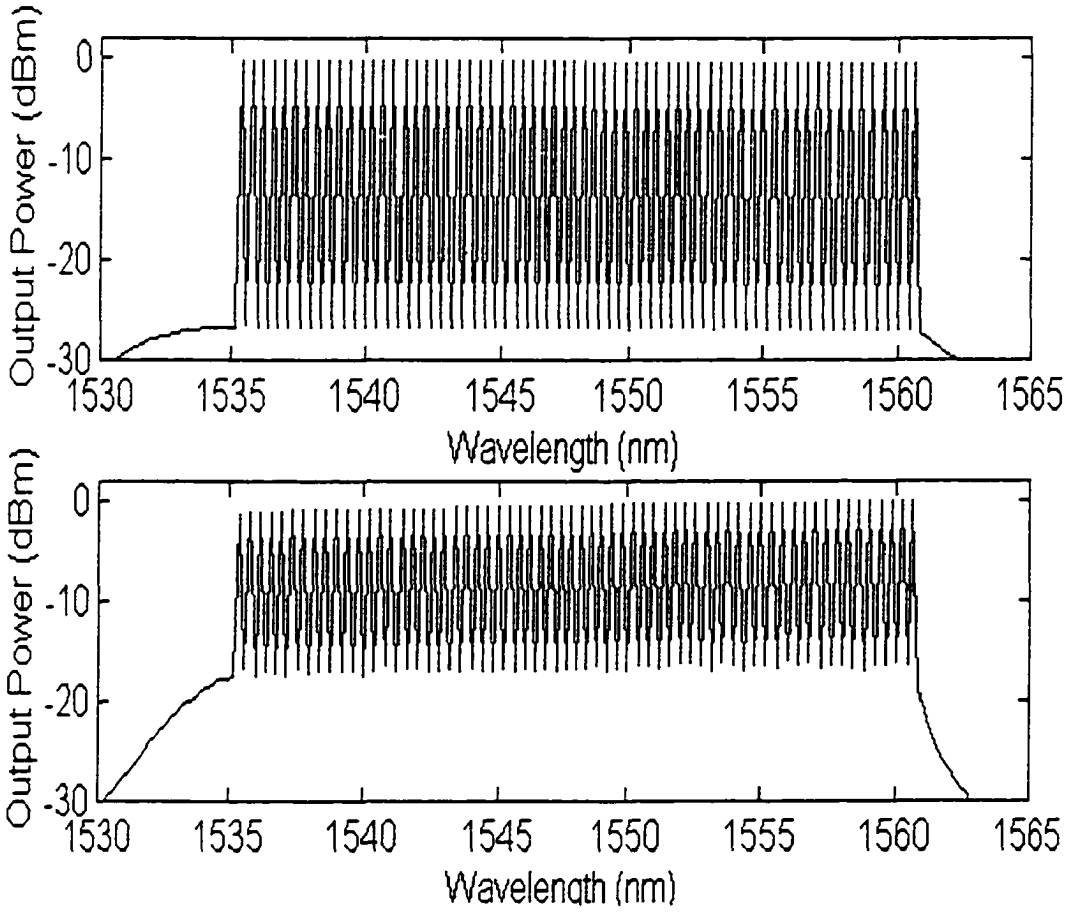

Figure 5.10. Spectra after 1st and 12th EDFA (0.2 nm resolution).

CHAPTER 6 *Conclusion*

6.1 Conclusion

This thesis has examined the technological requirements and has assessed the performance analysis and feasibility for implementing ultra-high bit-rate long-haul point-to-point transmission system based on Dense Wavelength-Division Multiplexing (DWDM) technology. Specifically, this work has developed and demonstrated several ultra-high bit-rate long-haul DWDM transmission system configurations. In these configurations, the number of DWDM channels varied from 16-100 wavelength at 622 Mb/s, 2.5 Gb/s and 10 Gb/s data rates per channel, giving total system capacities in the order of a Tb/s over a transmission distance of about 600-1200 km with 6-12 spans. To the best of our knowledge, this is the largest

DWDM Transmission systems with the highest capacity yet reported.

To realize an ultra-high speed long-haul DWDM transmission system, two key technological issues, that are the focus of this thesis, have been addressed:

- Novel architectures that offer a possible route to ultra-broad band amplifiers capable of providing 60-80 nm of optical bandwidth based on erbium-doped silica fiber have been developed. Using these ultra-broad band EDFAs, the number of WDM channels then grew to about 80-100 channels while keeping a channel spacing compatible with practical filtering technology.

This work has developed and demonstrated several novel two-band EDFA configurations capable of providing as large as 80-nm of optical bandwidth using only silica-based EDFAs. Such configurations offered a practical route to removing the bandwidth limits which currently constrain the design of flexible WDM systems and networks. With 80 nm of bandwidth, this EDFA configuration was able to accommodate 100 WDM channels with the proposed ITU standard channel spacing of 100 GHz. One of the most important criterion that was met in designing our proposed EDFA configuration is that it had to be flexible for graceful in-service upgrade to a maximum of 100 WDM channels along with the smooth evolution in increasing the bit rate per channel from OC-12 to OC-192.

Specifically, this work has investigated and developed several ultra wide-band gain-flattened and stabilized silica-based EDFA configurations with flexible and scalable Wavelength Add Drop (WADM) capabilities. The WADM was assumed to be located between the dual-stage EDFA of each band. Each WADM consists of fiber grating filters along with circulators and a given number of wavelength selective elements depending on the number of wavelengths to be added/dropped, to perform the WADM capabilities.

- A novel practical filtering technology that is compatible with the channel spacing has also been developed and investigated. Specifically, this thesis has compared and examined the potential of both existing and emerging WDM filtering technologies and developed a novel WDM filtering technologies using fiber grating filters.

In examining the filtering technology options, the characteristics of filters were compared based on the following:

- Insertion loss
- Optical bandwidth
- Crosstalk for both adjacent and non adjacent channels
- Polarization dependence loss

The proposed work was carried out in two overlapping phases: (i) modeling and simulation, and (ii) related experiments. First, we measured and characterized the performance of a single-stage/dual-stage amplifier. We also measured and fully characterized the performance of a single fiber grating filter by measuring its transmittance and reflectance transfer functions. Then, we have developed a flexible and user-friendly computer modeling tool to investigate the overall performance of several different two-band EDFA architectures with different pumping schemes, pumping wavelength, pumping power, and WADM capabilities. We then used the initial simulation results for guiding our experimental program, to establish theoretical limits to performance and to compare with experimental results.

The end-to-end performance of these two-band EDFA configurations were then tested and examined when cascaded in a practical ultra-high speed WDM backbone network. This was achieved in the context of modeling the end-to-end performance of several DWDM transmission systems. We have implemented a flexible, powerful computer modeling tool for evaluating the end-to-end performance of DWDM transmission systems. The tool included wavelength driven and time driven capabilities. The wavelength driven capability was required to model the effects of cascading many optical amplifiers and optical filters on the output signal to noise ratio and crosstalk level of any signal on the network. The time driven capability was required to model the effects of fiber chromatic and polarization dispersion, crosstalk from adjacent channels, timing jitters due to noise and crosstalk, and non-perfect

extinction ratio in external modulators, on the signal quality in the network. The model related parameters at the device-level to system-level performance measures such as bit error rate (BER) and noise margin.

Finally, using the key DWDM enabling technologies developed in this thesis, we have demonstrate and characterize the end-to-end performance of sixteen 2.5 Gb s DWDM channels transmission over 800 km of standard SMF.

CHAPTER 7

Bibliography

7.2 Chapter 1

[1] A. M. Vengsarkar, et al, J. of Lightwave Tech., vol.14, no.1, pp.58-65, January, 1996.

[2] A. K. Srivastava, et al, Proc. of OFC'97, Dallas, TX, PD 18, February , 1997.

[3] P. F. Wysocki, et a, "Erbium-doped fiber amplifiers flattened beyond 40 nm using long-period grating", Proc. of OFC'97 Post-deadline paper PD2, Dallas, TX, PD2, February , 1997.

[4] S. Artigaud et al., "Transmission of 16 x 10 Gb/s channels spanning 24 nm over 531 km of conventional single-mode fiber using 7 in-line fluoride-based EDFAS", Proc. of OFC'96

Post-deadline Paper PD27, San Jose, Cal., 1996.

[5] A. Mon, et al, Proc. of OFC, Dallas, TX, PDl, February , 1997.

[6] J. F. Massicott, et al, Elect. Lett., vol.28, no.20, pp.1924-1925, September,1992.

[7] H. Ono, et al, IEEE Photon. Tech. Lett., vol.9, no.5, pp.596-598, May, 1997.

7.3 Chapter 2

[1] F. Shehadeh, Survivable and scaleable multiwavelength ring network architectures for broad-band fiber optic networks: An experimental demonstration, 1997.

[2] Olsson, N. A. (1989). Lightwave systems with optical amplifiers. *J. Lightwave Technol.*, 7, 1071-1082.

[3] Marcuse, D. (1990). Derivation of analytical expressions for the bit-error probability in lightwave systems with optical amplifiers. *J. Lightwave Technol.*, **8**, 1816-1823.

[4] Fishman, D. A., Duff, D. G., Nagel, J. A. (1990). Measurement and simulation of multi-path interference for 1.7 Gb/s lightwave transmission systems using single-and multifrequency lasers. *J. Lightwave Technol.*, Vol. **8**, 894-905.

[5] Kuo, C. Y., Kao, M. L., French, J. S., Tench, R. E., and Cline, T. W. (1990). 1.55 μ m, 2.5 Gb/s direct detection repeaterless transmission of 160 km non-dispersion shifted fiber. *IEEE Photon. Technol. Lett.*, **2**, 911-913.

[6] Reichmann, K., Magill, P. D., Koren, U. Miller, B. I., Young, M., Newkirk, M., and Chien, M. D. (1993). 2.5 Gb/s transmission over 674 km at multiple wavelengths using a tunable DBR laser with an integrated electroabsorption modulator. *IEEE Photon. Technol. Lett.*, 5,1098-1100.

[7] Fishman D. A. (1993). Design and performance of externally modulated 1.5 - μm laser transmitter in the presence of chromatic dispersion. *J. Lightwave Technol.* **11**, 624-632.

[8] Ogata, T., Nakaya, S., Aoki, Y., Saito, T., and Henmi, N. (1992). Long-distance, repeaterless transmission utilizing stimulated Brillouin scattering suppression and dispersion compensation. 4th *Optoelectronics Conference, Makuhari Messe, Japan*. paper 16A4-3.

[9] Suzuki, N. and Ozeki, T. (1993). Simultaneous compensation of laser chirp, Kerr effect, and dispersion in 10 Gb/s long-haul transmission systems. *J. Lightwave Technol.*, **11**, 1486-1494.

[10] Linke, R. A. (1985). Modulation induced transient chirping in single frequency lasers. *IEEE J. Quantum Electron.*, **21**, 593-597.

[11] Kataki, Y., and Soda, H. (1995). Time-resolved chirp measurement of modulator-integrated DFB LD by using a fiber interferometer. Conference on Optical Fiber Communication (OFC'95). paper FC4.

[12] Fells, J. A. J., Gibbon, M. A., Thompson, G. H. B., White, I. H., Penty, R. V., Wright, A. P., Saunders, R. A., Armistead, C. J., and Kimber, E. M. (1995). Chirp and system performance of integrated laser modulators. *IEEE Photon. Technol. Lett.*, November 1995.

[13] Sessa, W. B., and Wagner, R. E. (1992). Frequency stability of DFB lasers used in FDM multi-location networks. *Conference on Optical Fiber Communication (OFC '92)*, paper ThC3.

[14] Vodhanel, R. S., Krain, M., Wagner, R. E., and Dessa, W. B. (1994). Long-term wavelength drift of the order of -0.01 nm/yr for 15 free-running DFB laser modules. *Conference on Optical Fiber Communication (OFC '94)*, paper WG5.

[15] Chung, Y. C., Jeong, J., and Cheng, L. S. (1994). Aging induced wavelength shifts in 1.5 μ m DFB lasers. *IEEE Photon. Technol. Lett.* , **6**, 792-795.

[16] Kaminow, Koch. (1997). *Optical fiber communication IIIB*.85-87.

[17] Takahashi, H., Susuki, S., Kato, K., and Nishi, I. (1990). Arrayed-waveguide grating for wavelength division multi/demultiplexer with nanometer resolution. *Electronics letters*, vol. 26 No. 2.

7.4 Chapter 3

[1] Laser Focus World. March 1997.pg 111.

[2] Yuan P. Li and Leonard G. Cohen. "Planar waveguide DWDMs for telecommunications: Design tradeoffs". August 4, 1997.

[3] D. Fishman and M. Spector. "Wavelength tolerance with 100 Ghz spacing". March 1997.

[4] F. Shehadeh, "Survivable and scalable multiwavelength ring network architectures for broad-band fiber optic networks: An experimental demonstration", 1997.pg. 31.

[5] M. A. Scobey and D. E. Spock, "Passive DWDM components using Microplasma optical interference filters",OFC'96, paper ThK1, San Jose, Feb. 1996.

[6] I. Kaminow and T. Koch. "Optical Fiber Telecommunications IIIB",1997. pg. 274.

7.5 Chapter 4

[1] A. K. Srivastava et al., "32 x 10 Gb/s transmission over 640 km using broad band, gain-flattened erbium-doped silica fiber amplifiers", OFC'97 Post-deadline paper PD18, Dallas, Texas, 1997.

[2] [2] Neal S. Bergano et al., "Long-Hual transmission using optimum channel modulation: A 160 Gb/s (32 x 5 Gb/s) 9,300 km demonstration", OFC'97 Post-deadline Paper PD16, Dallas, Texas, 1997.

7.6 Chapter 5

[1] A. M. Vengsarkar, et al, J. of Lightwave Tech., vol.14, no.1, pp.58-65, January, 1996.

[2] A. K. Srivastava, et al, Proc. of OFC'97, Dallas, TX, PD 18, February , 1997.

[3] P. F. Wysocki, et a, "Erbium-doped fiber amplifiers flattened beyond 40 nm using long-period grating", Proc. of OFC'97 Post-deadline paper PD2, Dallas, TX, PD2, February, 1997.

Photon. Tech. Lett., vol.9, no.5, pp.596-598, May, 1997.

[4] Strasser, T. A., "Bragg gratings, photosensitivity, and poling in glass fibers and wave guides: applications and fundamentals", Williamsburg, Virginia, PD2A, October 26-28, 1997.

[5] M. A. Ali, R. E. Wagner, A. Elrefaie, and S. Ahmed "A detailed comparison of the overall performance of 980- and 1480-nm pumped EDFA cascades in WDM multiple access Light-wave networks," J. Lightwave Technology, Vol. 14, PP. 1436-1448, June 1996.

[6] M. Mendez and M. A. Ali, "Simulation of 64 x 2.5 Gb/s WDM Transmission Over 1056 km of Standard Single Mode Fiber Using Gain-flattened Silica-Based EDFAs," IEEE Photon-ics Technology Letters, Vol. 10, PP. 300-302, Feb. 1998.

[7] C. R. Giles and E. Desurvire, "Modeling erbium-doped fiber amplifiers," J. Lightwave Technology, Vol. 9, pp. 271-283, 1991.

[8] D. Marcuse, "Derivation of analytical expressions for the bit-error probability in lightwave systems with optical amplifiers," J. Lightwave Technol., Vol. 8, No, 12, pp. 1816-1823, 1990.

[9] A. K. Srivastava et al., "32 x 10 Gb/s transmission over 640 km using broad band, gain-flattened erbium-doped silica fiber amplifiers", OFC'97 Post-deadline paper PD18, Dallas, Texas, 1997.

[10] Neal S. Bergano et al., "Long-Hual transmission using optimum channel modulation: A 160 Gb/s (32 x 5 Gb/s) 9,300 km demonstration", OFC'97 Post-deadline Paper PD16, Dallas, Texas, 1997.

[11] S. Artigaud et al., "Transmission of 16 x 10 Gb/s channels spanning 24 nm over 531 km of conventional single-mode fiber using 7 in-line fluoride-based EDFAS", OFC'96 Post-deadline Paper PD27, San Jose, Cal., 1996.

[12] J. Pan, M. A. Ali, A. Elrefaie, and R. Wagner, "Multiwavelength Fiber-Amplifier Cascades with Equalization employing Mach-Zehnder optical filter," IEEE Photonic_Technology Letters, Vol. 7, PP. 1501-1503, Dec. 1995.

IMAGE EVALUATION TEST TARGET (QA-3)

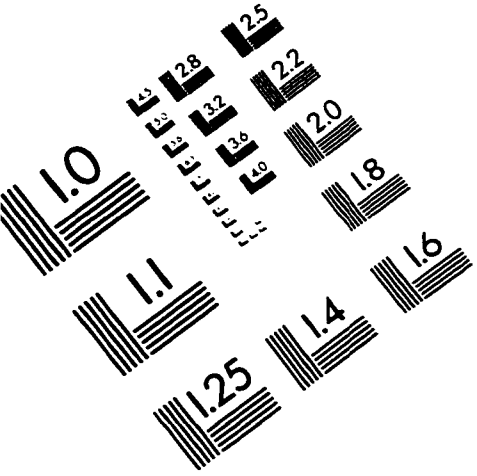

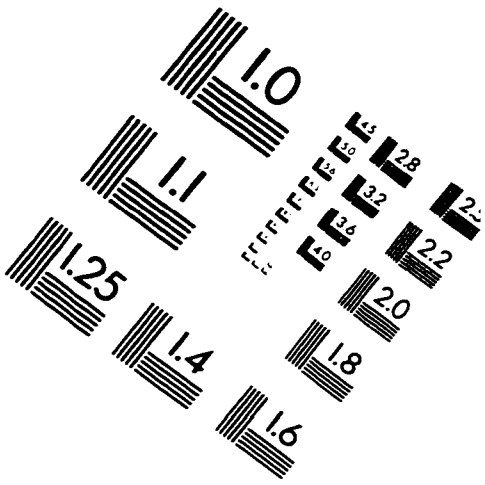

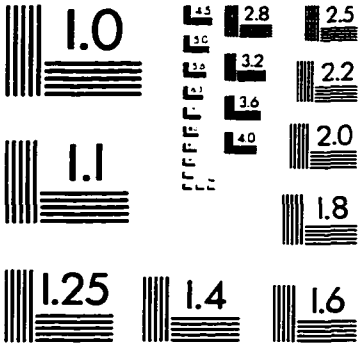

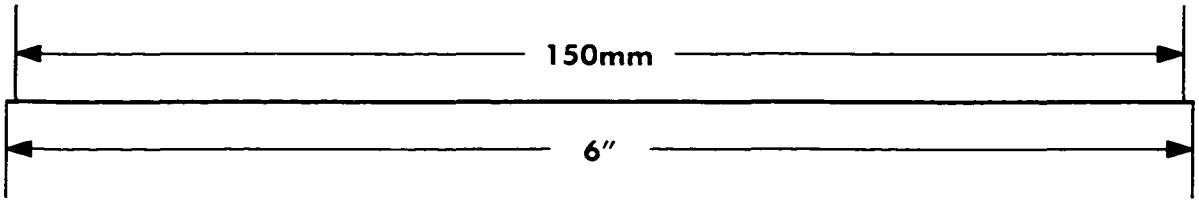

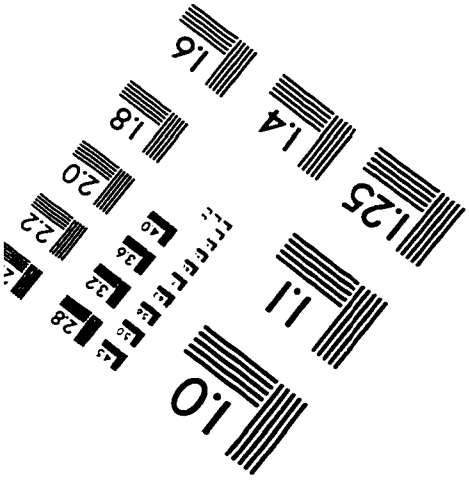

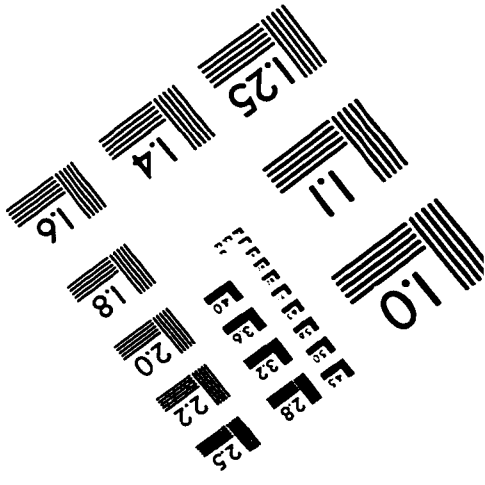

APPLIED IMAGE, Inc
1653 East Main Street
Rochester, NY 14609 USA
Phone: 716/482-0300
Fax: 716/288-5989